Project B.14 – Demonstration of Enhanced Fire Safety Technology – Fire Suppression Systems

Part 2B: Evaluation of a Fire Suppression System in a Full Scale Vehicle Crash Test and Static Vehicle Fire Tests – Underbody Gasoline Fires

Jeffrey Santrock
General Motors Corporation

and

Steven E. Hodges
Santa Barbara, California

Abstract

This report describes tests of an experimental fire suppression system installed on the underbody of a test vehicle. The experimental fire suppression system consisted of two Solid Propellant Gas Generators (SPGG) and two optical detectors. The test vehicle was subjected to a crash test that, in a previous test, resulted in a leak in the fuel tank. No fuel leak and no fire occurred in the crash test conducted for the study described in this report. A series of six static fire tests of this experimental fire suppression system in the crash tested vehicle were conducted after this crash test. The ignition protocols used in these tests involved pumping gasoline from an external reservoir onto the top of the fuel tank in the test vehicle. The gasoline was allowed to run onto the ground under the test vehicle and ignited with a high-voltage electrical discharge. In some of these static fire tests, additional gasoline was poured onto the ground around the test vehicle before ignition. This experimental fire suppression system used in these tests extinguished the test fires in two of six tests.

Table of Contents

Appendicies

List of Figures

Report

List of Figures

Appendicies

List of Tables

Report

1 Introduction

The tests described in this report were conducted by General Motors (GM) pursuant to an agreement between GM and the U.S. Department of Transportation. The purpose of these tests was to evaluate the effects of on-board fire suppression systems in post-crash vehicle fire tests. An experimental fire suppression system based on optical fire detection and Solid Propellant Gas Generator (SPGG) fire suppressant technology was installed on the underbody of a test vehicle (1999 Honda Accord). The test vehicle was then subjected to a crash test using a test protocol that resulted in fuel leaking onto the ground under the rear of a similar test vehicle in a previous crash test [1]. The cause of the fuel leak in that previous test was determined to be a compromised fuel tank and fuel sender [1]. After the crash test conducted for the current investigation, a series of static fire tests using the crash-tested vehicle were conducted where fires under the rear of the underbody were staged to further evaluate this system. The ignition scenario used in these static fire tests included ignition of gasoline under the rear portion of the crash-tested vehicle using a high voltage electric arc.

The criteria for assessing the effectiveness of the fire suppression system in the event of a fire during the crash test and during the subsequent fire tests were: (i) if the fire suppression system remained functional during and after the crash test and (ii) if the fire suppression system extinguished a fire under the rear of the vehicle in the post-collision static fire tests. The rational for selecting fire suppression systems based on SPGG technology for the tests described in this report is discussed in Section 3. The intent of the using the crash tested vehicle in a series of static vehicle fire tests was to examine the performance of this type of fire suppression system under different fire scenarios in the rear underbody of a post-collision vehicle

2 Crash Test

The rear crash test (C12611) occurred on August 17th 1999. The vehicle used in this test was stationary, and was impacted in the left rear by a moving barrier fitted with a deformable aluminum honeycomb face similar to that described in FMVSS 214. The mass of the test vehicle was 1649.0 kg (1043.0 kg front and 606.0 kg rear).[1] The trajectory of the barrier (velocity vector) of the barrier was parallel to the longitudinal mid-line of the vehicle. The mass of the moving barrier was 1365.0 kg. The barrier speed at impact was 85.0 km/hr. The target overlap between the barrier face and the rear of the test vehicle was 70% on the left side of the test vehicle. The

[1] The test vehicle contained two 50th percentile adult male anthropomorphic body forms in the front seating positions for ballast. The mass of each ATD was 75.7 kg. No data were recorded from the anthropomorphic body forms during either test.

horizontal center-line of the simulated bumper on the barrier face was aligned with the horizontal centerline of the bumper beam in the test vehicle.

The crash test setup is illustrated schematically in Figure 1. Figure 2 is a photograph of the test vehicle and barrier before this crash test showing the alignment of the vehicle relative to the barrier.

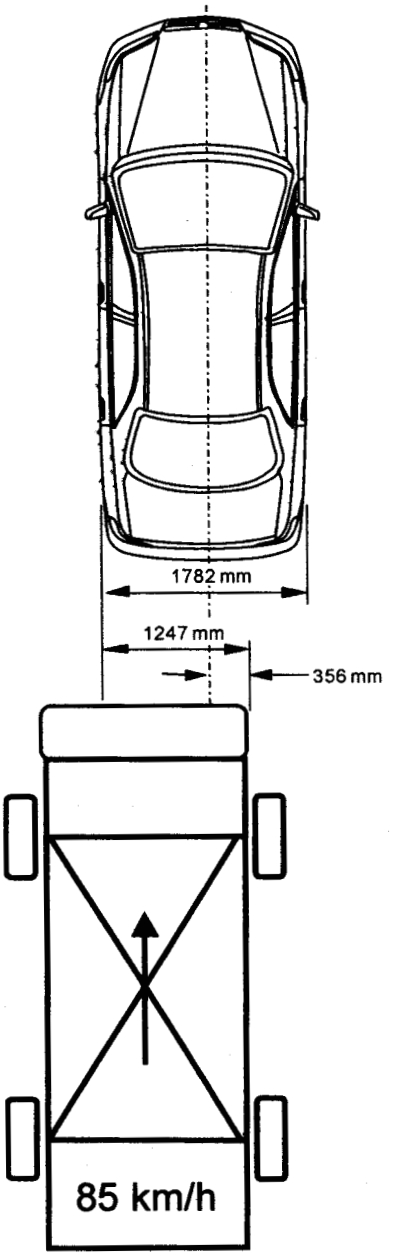

Figure 1. Crash test set-up for C12611.

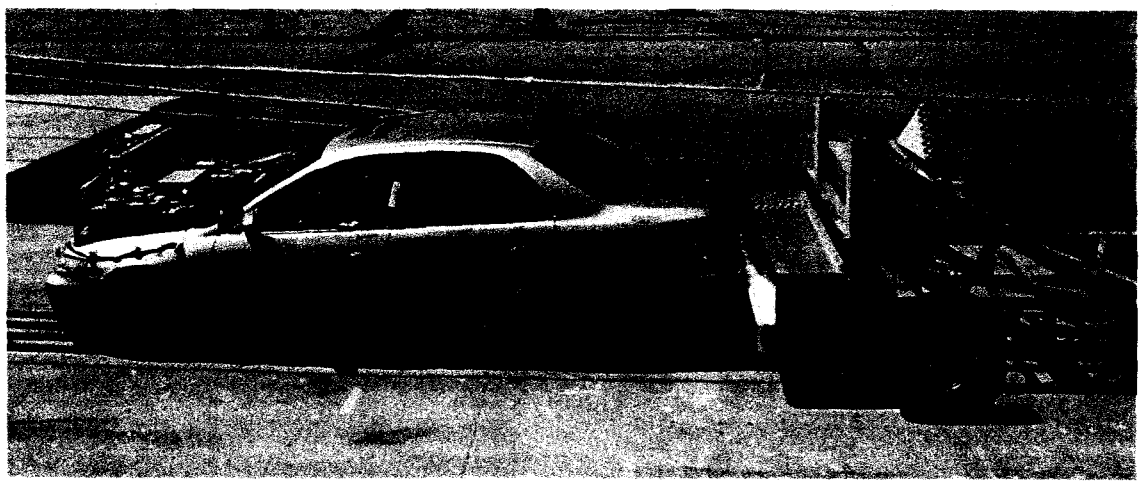

Figure 2. Crash Test C12611. Photograph showing the alignment of the barrier relative to the test vehicle before this test.

The test vehicle contained the factory fills of motor oil (5.6 L), transmission fluid (6.2 L), engine coolant (6.9 L), brake fluid (capacity unknown), power steering fluid (1.1 L), and windshield washer fluid. The fuel tank in the test vehicle contained approximately 61 L of regular unleaded gasoline. To achieve engine compartment, exhaust system, and fuel system temperatures representative of some driving conditions, a pre-impact warm-up schedule was followed in which the test vehicle was idled with an engine speed of 1500 to 1800 rpm for approximately 45 minutes before impact. At impact, the ignition in the test vehicle was on and the engine speed was approximately 1750 rpm; the transmission was in neutral; the brakes were on; the radio was on; the Hi-beam headlights were on; the left turn signal was on; and the rear window defogger was on. Figure 3 shows the crash test vehicle before and after this crash test.

2.1 Crash Test Summary

Data recorded from accelerometers located on the rocker panels is contained in Appendix A. Data recorded from the flammable vapor sensors is in Appendix B. Samples for gas chromatography / mass spectroscopy analysis were not acquired during this crash test. Exhaust system temperature data is in Appendix D. Fire suppression system data is in Appendix E.

Crash Test C12611 did not result in a fuel leak in the test vehicle and no fire was observed during this crash test. Neither SPGG unites activated during this crash test. Figure 4 shows close-up views of the optical detectors and SPGG units on the underbody of the test vehicle after this crash test.

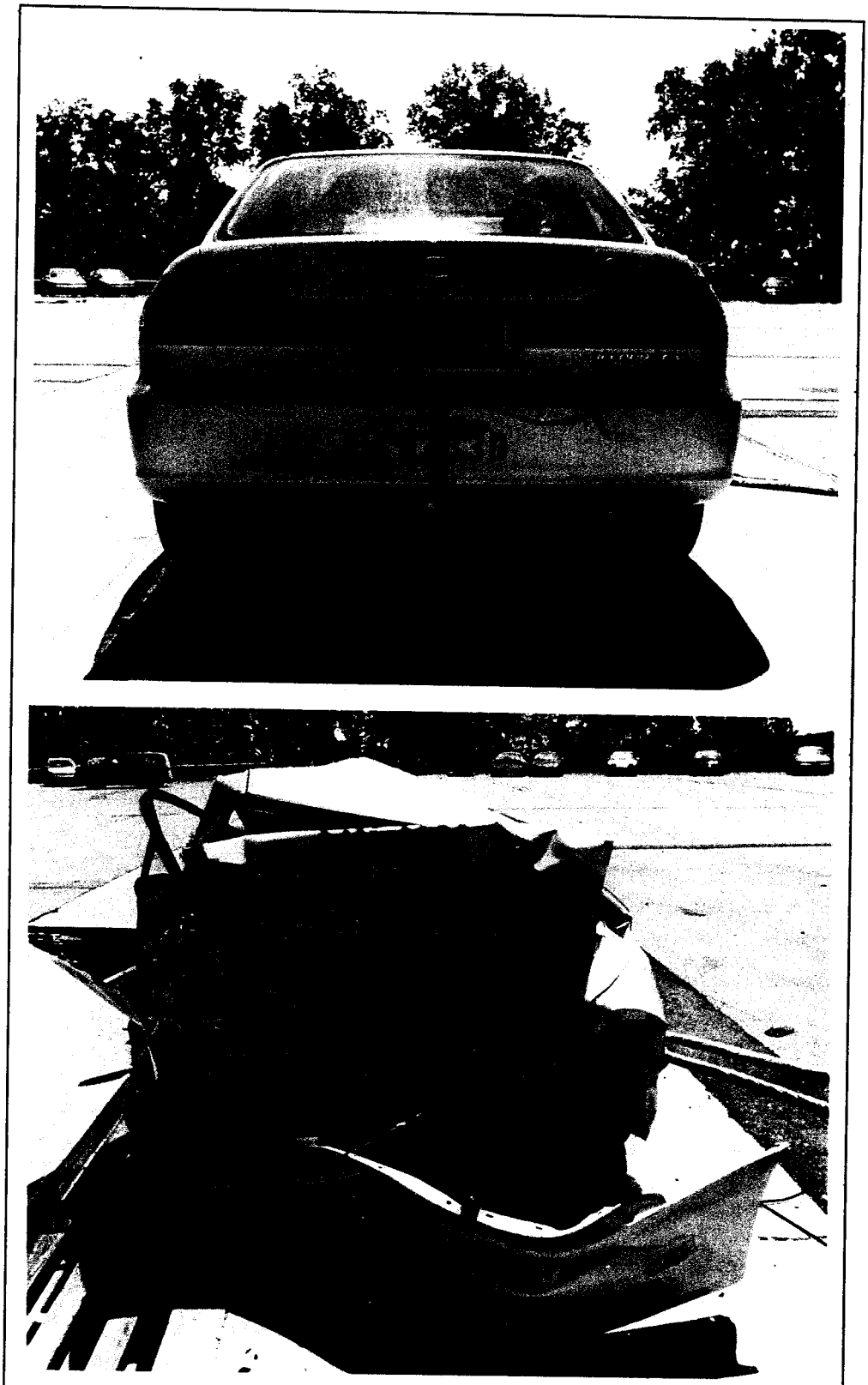

Figure 3. Crash Test C12611. Photographs of the test vehicle before (upper) and after (lower) this crash test.

- The flammable vapor sensor data and GC / MS data from this crash test did not detect gasoline vapor during this crash test (Appendix C).

- Surface temperatures of the exhaust system were not sufficient to result in autoignition of gasoline at the time of impact and for 5 minutes after impact (Appendix D).

- No evidence of a fuel system leak or fire was observed during and immediately following the crash test, in the high-speed film recorded of this crash test, or in physical inspection of the test vehicle after this crash test.

2.1.1 Vehicle Warm-up Timing

Table 1 summarizes the pre-impact warm-up schedules for the test vehicle.

Table 1
Summary of Crash Test Countdown

0:00	Start Engine
0:01	Radio – On
0:02	Set Idle to 1500 rpm Left Turn Signal – On High Beam Head Lights – On
0:23	Idled Check: 1750 rpm
0:28	Gas Sensor Electronics – Off
0:30	Begin Instrumentation Set-Up
0:33	End Instrumentation Set-Up
0:35	Gas Sensor Electronics – On Transmission to Neutral Parking Brake – Off
0:35	Begin Countdown

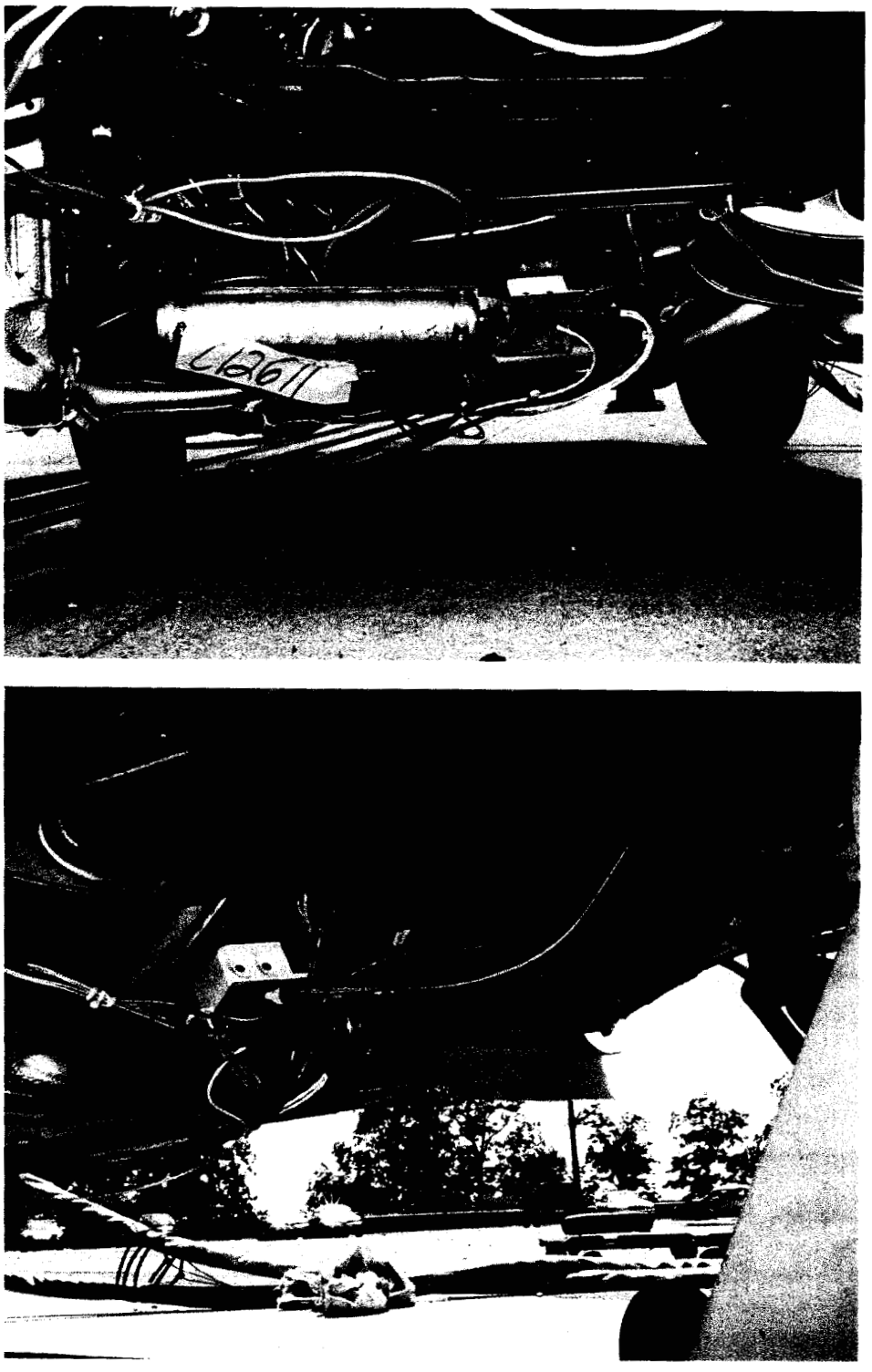

Figure 4. Crash Test C12611. Photographs of the optical detectors and SPGG units mounted on the underbody of the test vehicle after this cash test.

2.1.2 Vehicle Mass, Barrier Mass, and Impact Parameters

The test vehicle's front, rear, and total mass, as well as the barrier's total mass, speed at the time of impact, and place of impact are summarized in Table 2.

Table 2
Test Vehicle Mass, Barrier Mass, Barrier Velocity, and Location of Impact

	Test Data
Vehicle Test Mass – Front	1048.0 kg
Vehicle Test Mass – Rear	600.0 kg
Vehicle Test Mass – Total	1648.0 kg
Barrier Mass	1670.0 kg
Barrier Velocity at Impact	85.0 km/hr
Location of Impact	Impact at test vehicle's rear with a left overlap of 1247 mm.

2.1.3 Accelerometer Data

Five tri-axial (longitudinal, lateral, and vertical) accelerometers were mounted to each of the test vehicles in the following locations: Right front rocker panel; Left front rocker panel; Right Rear Rocker Panel; Left Rear Rocker Panel; Rear Underbody Floor pan at Fire Sensor. Each of these sensors recorded acceleration, velocity, and displacement.

Data recorded from the accelerometers on the left and right front rocker panels indicated that the average change in velocity of the test vehicle was 40.8 km/h in the longitudinal direction and 5.8 km/h in the lateral direction, indicating a slight clockwise rotation of the test vehicle (**APPENDIX A**). The accelerometers on the rear rocker panels were in the crush zone. Because measurements obtained from these accelerometers were affected by vehicle crush during the crash test, data from these accelerometers were not used to calculate the change in velocity of the test vehicle.

2.2 Flammable Vapor Sensors

Five flammable gas sensors (TGS 813, FIGARO USA, Inc, Wilmette, IL) were installed in the engine compartments of the test vehicle. Flammable gas sensors were in the following locations in the test vehicle. Gas Sensor S1 was located at the right side of the rear cross member in the fuel tank / rear axle assembly. Gas Sensor S2 was located at the center of the rear cross member in the fuel tank / rear axle assembly. Gas Sensor S3 was located at the left side of the rear cross member in the fuel tank / rear axle assembly. Gas Sensor S4 was located adjacent to the catalytic converter. Gas Sensor S5 was located above the fuel tank.

Gas phase concentration – sensor output voltage calibration data was obtained using heptane in the range of 0 to 5% (V/V). The tin oxide semiconductor elements in these sensors also respond to changes in temperature. Changes in the air temperature around one of these sensors or changes in airflow over one of these sensors can result in small changes in the output voltage.

2.2.1 Flammable Vapor Data

Data recorded for S1 and S2 showed no increase in sensor output from pre-impact levels (Plots B1 and B2, **APPENDIX B**). Data recorded from S3, S4, and S5 showed increases in sensor voltage outputs equivalent to ≤ 0.02% (V/V) heptane in air. These fluctuations in voltage output are consistent with either (1) hydrocarbons and other flammable gases in the space below the rear of the test vehicle in concentrations substantially less than the lower limit of flammability, or (2) changes in sensor temperature or airflow.

2.3 Gas Chromatography / Mass Spectroscopy Analysis of Engine Compartment Air Samples

Samples for gas chromatography / mass spectroscopy analysis were not acquired during this test.

2.4. Crash Test Temperature Data

Five thermocouples were installed in the test vehicle for this crash test. Thermocouple TC1 was intrinsically welded to the lower surface of the exhaust system resonator. Thermocouples TC2 and TC3 were intrinsically welded to Exhaust Pipe B. Thermocouple TC4 was intrinsically welded to the lower surface of the muffler. Thermocouple TC5 was a shielded thermocouple located near the rear surface of the resonator.

2.4.1 Component Temperature Data

Appendix D contains plots of data recorded from thermocouples during this crash test. Table 3 shows temperatures recorded from these thermocouples at the time of impact. Temperatures recorded from all thermocouples decreased after impact.

Table 3
Component Temperatures Recorded at Impact

Thermocouple / Location	Temperature
Thermocouple 1 Exhaust Resonator	74°C
Thermocouple 2 Exhaust Pipe B	156°C
Thermocouple 3 Exhaust Pipe B	174°C
Thermocouple 4 Muffler	114°C
Thermocouple 5 Rear Underbody Air	49°C

2.5 Crash Test Fire Suppression System

The fire suppression system installed in the test vehicle for this test included two solid propellant gas generator fire suppression units and two optical flame detectors. Both SPGG units and optical flame detectors were mounted to the floor panel in the "kick-up" area for the rear seat cushion. Each SPGG unit was attached to an aluminum bracket using two adjustable hose clamps. The aluminum brackets were bolted to the floor panel just inboard of the left and right rocker. Each bracket contained a curved shield to direct the effluent from the SPGG unit toward the rear of the test vehicle and a platform for one optical flame detector. The optical flame detectors were aimed toward the rear of the test vehicle and angled downward approximately - 5° relative to the plane of the floor panel. The optical detectors used in this test had a minimum 90° conical optical field of view and were designed to detect a hydrocarbon flame.

Deformation of the test vehicle in this crash test caused the orientation of the optical detectors and SPGG units to change (see Fig. 4). Both optical detectors were tilted upward, with the optical detector on the left side of the test vehicle tilted upward approximately 60°.

3 Evaluation of the Selected SPGG Fire Suppression System

Fire suppression systems based on solid propellant gas generator technologies were selected for the tests described in this report based on (1) the results of testing conducted by the Building and Fire Research Laboratory, National Institutes of Standards and Technologies (BFRL/NIST) and (2) evaluation of system characteristics in proposals received from suppliers of fire suppression systems that, in principle, could be adapted for use in motor vehicles. In a separate testing program, researchers at the BFRL / NIST evaluated a number of fire suppression technologies in small- and large-scale laboratory tests. These tests examined the effectiveness of gaseous fire suppression agents, dry chemical fire suppression agents, and SPGG fire suppression systems in a number of laboratory fire scenarios. The results of the BFRL/NIST testing program indicated the following order of effectiveness for the three types of technologies tested: SPGG systems > dry chemical agents > gaseous agents [2].

Fire Protection Systems designed to be integrated onto a vehicle have become commonplace for larger vehicles, such as transit buses [3]. Systems for smaller automobiles are not widely available. Proposals from four suppliers were evaluated to select a fire suppression system for the tests described in this report. Two of these proposals described fire suppression systems based on optical flame detectors and some type of dry chemical agent contained in one or more pressurized reservoir. Two proposals described fire suppression systems based on optical flame detectors and SPGG units. Dry chemical weight density flow rate concentrations (mass/protected volume/sec) of approximately 3 $kg/m^3/s$ (0.2 $lb/ft^3/s$) are required to suppress or extinguish a fire. This concentration must be maintained long enough so that reflash does not occur [4]. The required duration of the agent discharge will depend on application details, i.e., maximum delay between a fire alarm and the stoppage of air flow, time from collision to coming to rest, and so on [5]. The proper performance of dry chemical fire extinguishing systems depends critically on good design and correct system installation. Critical parameters include discharge nozzle quantity and location, agent distribution length, and, of course, amount of agent [6]. Discharge durations for onboard vehicle fire extinguishers range from 10 sec for small vehicles with protected volumes of less than about 1 m^3, to more than 30 sec for larger protected volumes.

On-board vehicle automatic fire suppression systems are limited in the amount of suppression agent available by the intrinsic size and volume limitations of the protected vehicle. In designing

a fire suppression system, the minimum amount of agent required for a specific application is estimated based on the anticipated fire threat and, critically, by the volume of the area protected. The success of automatic fire protection systems in protecting military armored vehicles, transit buses and mobile mining equipment is based on the fact that the geometry of the protected area is essentially unchanged when a fire occurs. Therefore, the system is most effective if parameters, such as the volume of the protected space, used to pre-engineer the suppression system (i.e., used to determine agent quantity and distribution) do not change. The geometry of a post-collision vehicle is drastically and significantly altered by the crash. Statistical variations in comparing different crash scenarios typically are larger than the tolerance on the volume estimate of the protected space of the pre-engineered fire suppression systems. The result is that the system effectiveness cannot be guaranteed with anywhere near the certainty that can be had with similar systems applied on large or off-road vehicle where mechanical distortion and fire threat are not as correlated.

Fire suppression systems based on SPPG technology use a solid propellant similar to that used in air bag inflators to produce a mixture of inert gases and particulate that is propelled onto the fire in a high velocity gas discharge. Fire suppression can occur as a result of one or a combination of four mechanisms [7]. The inert gases released from the SPGG units displace air and reduce the supply of oxygen to the flame. Expansion of the inert gases reduces the total energy and thus the temperature of the flame, the Joule–Kelvin effect [8]. The residue from the propellant forms an aerosol in the effluent from the SPGG and, depending on the chemistry of gas generation from the solid propellant, this residue may have fire suppression properties similar to dry chemical agents. Finally, the high velocity discharge of gases from the SPGG unit can result in separation of the flame from the fuel source.

The fire suppression system used in this test was tested as received from the supplier without modification. Technical personnel from General Motors installed the optical flame sensors, inert SPGG units, and cabling in the test vehicle following instructions supplied by the supplier. Just before each test described in this report, active SPGG units were installed in the test vehicle by technical personnel from the supplier. Technical personnel from the supplier performed a final systems check to ensure that the system was functioning within specifications before the test.

The fire suppression system tested here consisted of two SPGG units and two optical flame sensors. Figures E1 and E2 in APPENDIX E show the fire suppression system in the test vehicle. This fire suppression system was configured so that detection of fire by one or both of the flame sensors would trigger the discharge of both SPGG units. Technical personnel from General Motors worked with the supplier to determine mounting locations for each component in

the test vehicle to minimize the probability of damage or destruction of the fire suppression system during the crash test. A redundant system configuration was selected to provide some fire suppression capability if one or more of the system components were damaged or destroyed during the crash test. Spent or damaged components were replaced after the crash test.

The intent of the crash test was to determine the effectiveness of these fire suppression systems under the scenario of a rear crash resulting in a fuel system leak and subsequent fire in and under the test vehicle. In the test, the fire suppression system was installed on the underbody in the rear of the test vehicle. This test vehicle was stationary and was struck in the left rear by a moving barrier. The rationale for selecting a 1999 Honda Accords and the rear crash test protocol used in this test was as follows. A previous crash test of a 1998 Honda Accord using the same rear crash test protocol as used in the front crash test described in this report resulted in a leak in the fuel system of the test vehicle. The Honda Accord has the same body architecture for model years 1998 and 1999. No incendiary devices or other artificial means of causing a fire were used in these crash tests; therefore, there was no certainty that a fire would occur during the crash test.

After the crash test, multiple fire tests were conducted using the crash-tested vehicle where the severity of the fire was increased until the limit of effectiveness of the suppression system was reached. These tests are referred to as static fire tests to denote the lack of vehicle motion and changes in the vehicle structure (i.e., dynamic crush). Both SPGG units were checked for proper weight and squib continuity and the operation of the optical flame detectors were checked before each static fire test. These static fire tests used a high voltage electric discharge to ignite gasoline pumped from an external reservoir onto the ground under the test vehicle. The amount and distribution of gasoline on and under the test vehicle was varied in these tests.

Although the crash-tested vehicle was used for these static fire tests, these tests did not include a number of factors that may occur in an actual vehicle crash. These differences may lead to differences in the performance of an active fire suppression system. One example is vehicle motion. Vehicle motion during and after a crash may effect the distribution of fuel and other possible ignition sources in and around the vehicle. Vehicle motion creates airflow around and through the vehicle, which may affect both the pattern of distribution and concentration of fire suppression agent. As vehicle movement after a crash may involve both translation and rotation about one or more vehicle axes with changing accelerations, it is impossible to simulate airflow from this type of motion when the test vehicle is stationary. Another example is vehicle crush. The structural deformation that occurs during a crash can change the size and geometry of the engine compartment substantially, affecting how the fire suppression agent is distributed. As with

vehicle movement, these changes in the vehicle's structure are complex and impossible to simulate in a static test. Another difference between a vehicle in a static fire test and a vehicle in an actual crash is component temperature. During the static fire tests where the engine was not running, all components in the test vehicle were at ambient temperature. Whereas, during an actual vehicle crash (and the crash tests conducted here), the engine is running and components in the engine compartment and the exhaust system are at temperatures greater than the ambient temperature. The elevated temperature may affect both the flammability properties of the materials used in motor vehicles and the effectiveness of the fire suppression agent. It is impractical to simulate road-load temperatures in a stationary test vehicle, especially when the engine has been damaged in a crash test and is inoperable.

The criteria for assessing the effectiveness of the suppression systems were (i) the ability of the fire suppression systems tested in this study to remain functional after the crash test, (ii) the ability of the fire suppression systems tested in this study to extinguish fires, if any, that occurred during or after the crash tests, and (iii) the ability of the systems tested in this study to extinguish fires during the static tests.

3.1 Frontal Crash Test

This crash test did not result in a fuel leak or fire in the test vehicle. The fire suppression system did not activate during this crash test. A test of the fire suppression system by technical personnel from the supplier indicated that both optical detectors and both SPGG units were functional after this crash test.

3.2 Static Fire Tests

A series of six static fire tests were conducted using the crash tested vehicle. For the static fire tests, the vehicle was stationary and all components were at ambient temperature. The SPGG units were recharged with solid gas generant before each test. The optical flame sensors were tested before each test to determine if they functioned within specifications. The test involved exposing each sensor to a test flame and monitoring its output signal. In all of the static fire tests described below, the optical flame sensors were determined to be functioning within specifications prior to each test.

In these static fire tests, the fuel source was gasoline supplied to the test vehicle from a pressurized external reservoir and the ignition source was a high voltage electric arc created by an external high voltage transformer. The external reservoir was connected to a rubber tube with

a stainless steel over-braid. The outlet of the stainless steel tube was located on top of the fuel tank of the test vehicle. Liquid gasoline flowed from the tube downward on the rear section of the fuel tank and dripped onto the ground from the rear cross-member of the rear suspension / fuel tank assembly. The flow rate of gasoline was set by varying the initial head pressure in the external reservoir and measuring the outlet flow rate until the target flow rate was achieved. During the static fire tests, gasoline was allowed to flow for approximately 30 s before it was ignited by a high voltage electric arc.

3.2.1 Static Test F990819A

The flow rate of gasoline was approximately 1 liter per minute. Several unsuccessful attempts were made to ignite the gasoline with a high voltage electric arc. It was determined that airflow under the test vehicle caused by a 1 to 5 mph ground level wind, measured using an anemometer, prevented ignition. Barriers to block the wind were placed on the ground up-wind of the test vehicle. A high voltage electric arc was then used to ignite the vapor above the liquid gasoline on the ground under the test vehicle. The dry cell batteries connected to the fire suppression system for this series of tests did not have a sufficient charge to operate the fire suppression system. The batteries were replaced with a DC power supply for the remainder of tests in this series.

3.2.2 Static Test F990819B

The flow rate of gasoline was approximately 1 L/min. Vapor above liquid gasoline ignited approximately 28.1 s after the start of gasoline flow onto the ground under the test vehicle. Figure 5 shows plots of the output signals from Detector 1 and Detector 2 to the fire suppression system controller, and the fireing pulse from the fire suppression system controller to the SPGG units during this test.

Detector 1 output a detection signal to the fire suppression system controller approximately 450 ms after ignition. Detector 2 output a detection signal to the fire suppression system controller approximately 540 ms after ignition. The fire suppression system controller output a firing pulse to the SPGG units approximately 750 ms after ignition. Figure 6 shows a sequence of video stills from this test at 200 ms before ignition, 500 ms after ignition, 800 ms after ignition, and 25 s after ignition. This series of video stills shows that the effluent from the SPGG units extinguished the flames without re-ignition.

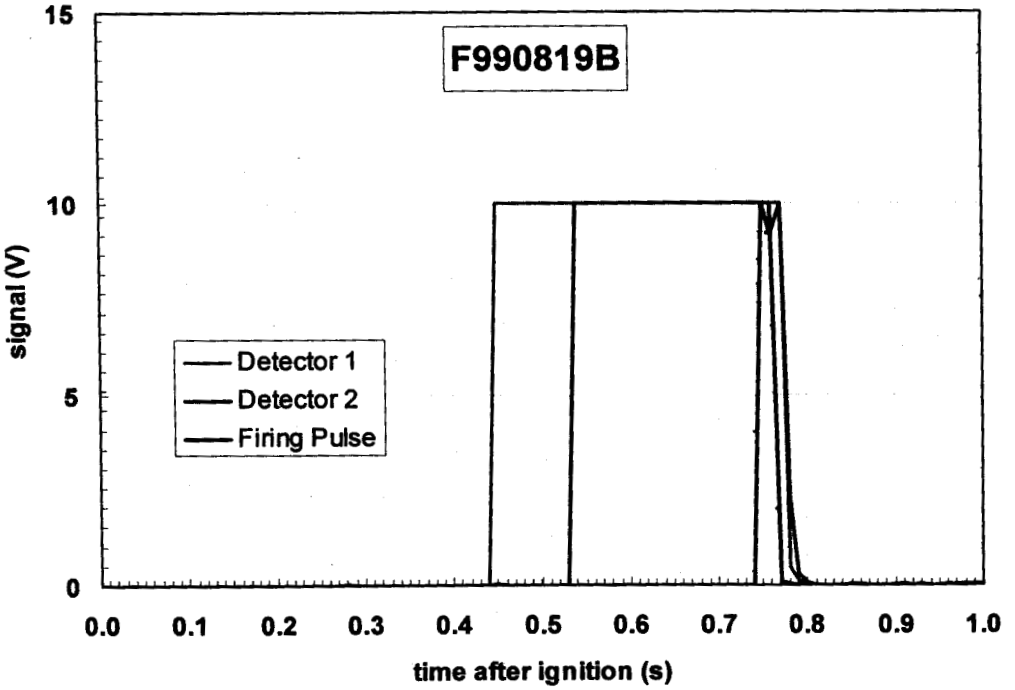

Figure 5. Static Fire Test F990819B. Plots of the output signals from Detectors 1 and 2 to the fire suppression system controller and the firing pulse from the fire suppression system controller to the SPGG units.

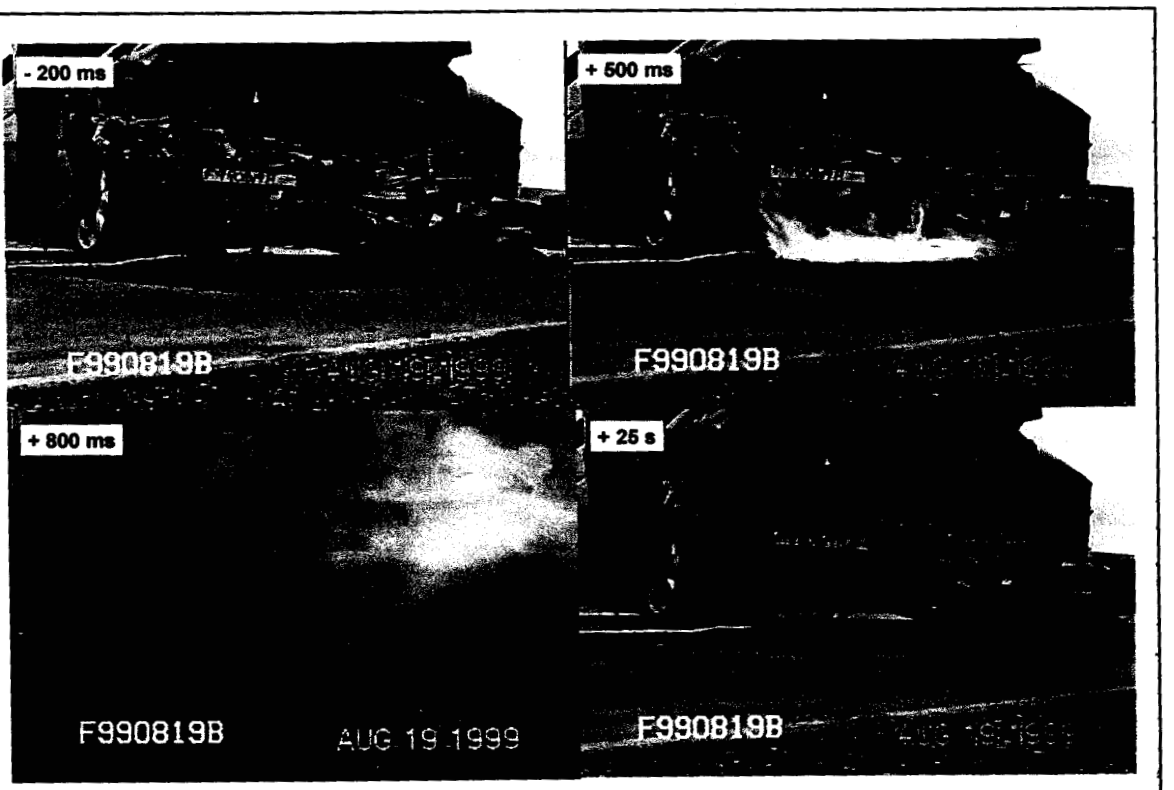

Figure 6. Static Fire Test F990819B. Video stills of this test at - 200 ms before ignition, and + 500 ms, + 800 ms, and + 25 sec after ignition.

3.2.3 Static Test F990819C

The flow rate of gasoline was approximately 2 L/min. Approximately 500 mL of liquid gasoline was poured onto the ground beyond (outboard) the left rear wheel of the test vehicle. Vapor above liquid gasoline ignited approximately 35 s after the start of gasoline flow onto the ground under the test vehicle. Figure 7 shows plots of the output signals from Detector 1 and Detector 2 to the fire suppression system controller, and the fire pulse from the fire suppression system controller to the SPGG units during this test.

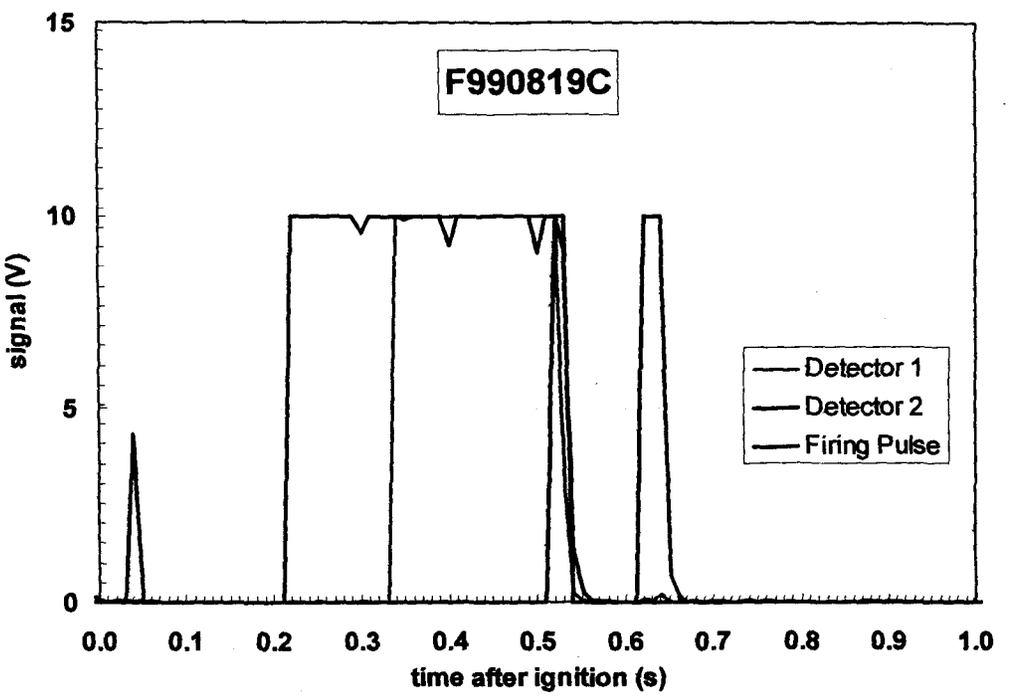

Figure 7. Static Fire Test F990819C. Plots of the output signals from Detectors 1 and 2 to the fire suppression system controller and the firing pulse from the fire suppression system controller to the SPGG units.

Detector 1 output a detection signal to the fire suppression system controller approximately 340 ms after ignition. Detector 2 output a detection signal to the fire suppression system controller approximately 220 ms after ignition. The fire suppression system controller output firing pulse to the SPGG units approximately 520 ms after ignition. Figure 8 shows a sequence of video stills from this test at 200 ms before ignition, 400 ms after ignition, 1000 ms after ignition, and 1500 ms after ignition. This series of video stills shows that the discharge from the SPGG units did not extinguish the fire. Gasoline outboard of the left rear wheel was shielded from the suppression

agent and continued to burn (arrow in Fig. 8), re-igniting liquid gasoline on the ground under the under the test vehicle after the SPGG discharge had ceased and airborne suppression agent was blown away from under the test vehicle. Safety personnel present for this test extinguished the fire using hand-held fire extinguishers (carbon dioxide).

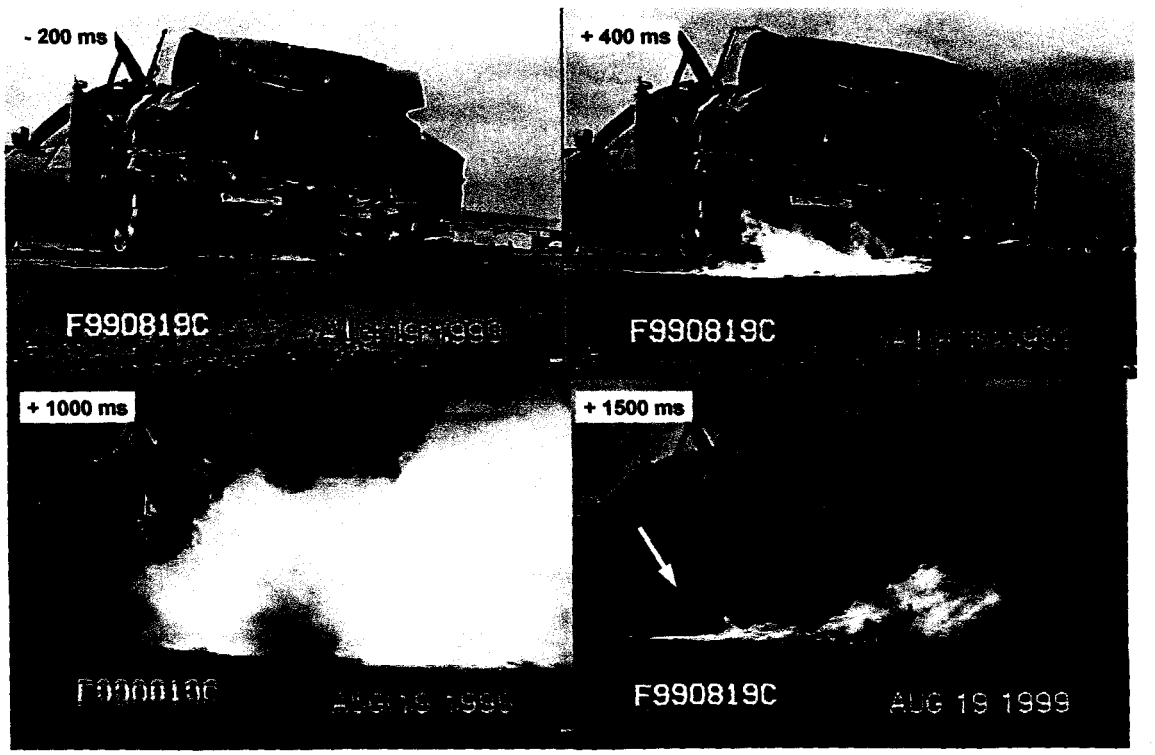

Figure 8. Static Fire Test F990819C. Video stills of this test at 200 ms before ignition (- 200 ms), 500 ms after ignition (+ 500 ms), 1000 ms after ignition (+ 1000 ms), and 1500 ms after ignition (+ 1500 ms).

3.2.4 Static Test F990820A

The flow rate of gasoline was approximately 3 L/min. Approximately 500 mL of liquid gasoline was poured onto the ground extending about 1000 mm behind the test vehicle. Vapor above liquid gasoline ignited approximately 18.9 s after the start of gasoline flow onto the ground under the test vehicle. Figure 9 shows plots of the output signals from Detector 1 and Detector 2 to the fire suppression system controller, and the fire pulse from the fire suppression system controller to the SPGG units during this test.

Detector 1 output a detection signal to the fire suppression system controller approximately 540 ms after ignition. Detector 2 output a detection signal to the fire suppression system controller approximately 630 ms after ignition. The fire suppression system controller output firing pulse to the SPGG units approximately 830 ms after ignition.

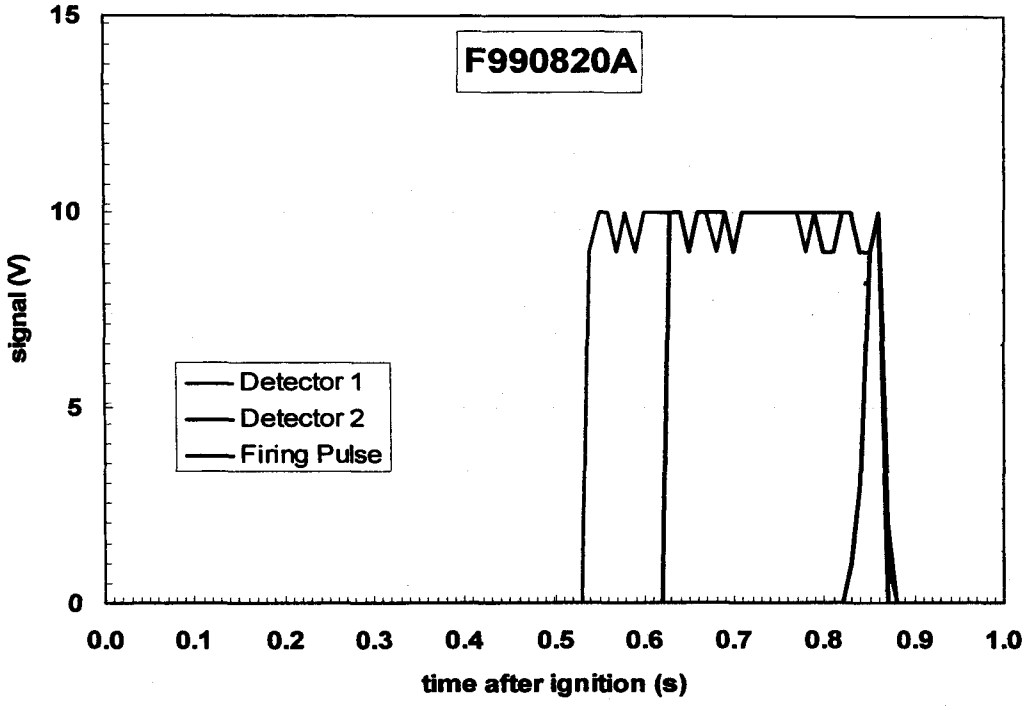

Figure 9. Static Fire Test F990820A. Plots of the output signals from Detectors 1 and 2 to the fire suppression system controller and the firing pulse from the fire suppression system controller to the SPGG units.

Figure 10 shows a sequence of video stills from this test at 200 ms before ignition, 500 ms after ignition, 800 ms after ignition, 1300 ms after ignition, and 6 s after ignition. This sequence of video stills shows that the discharge from the SPGG units did not extinguish the fire. Gasoline outboard of the muffler and exhaust pipes was shielded from the suppression agent and continued to burn after the SPGG discharge had ceased and airborne suppression agent cleared from under this section of the test vehicle (arrow in + 1300 ms video still in Fig. 10). Flames propagated from the shielded, unextinguished flame to gasoline on the ground under the under the test vehicle. Safety personnel present for this test extinguished the fire using hand-held fire extinguishers (carbon dioxide).

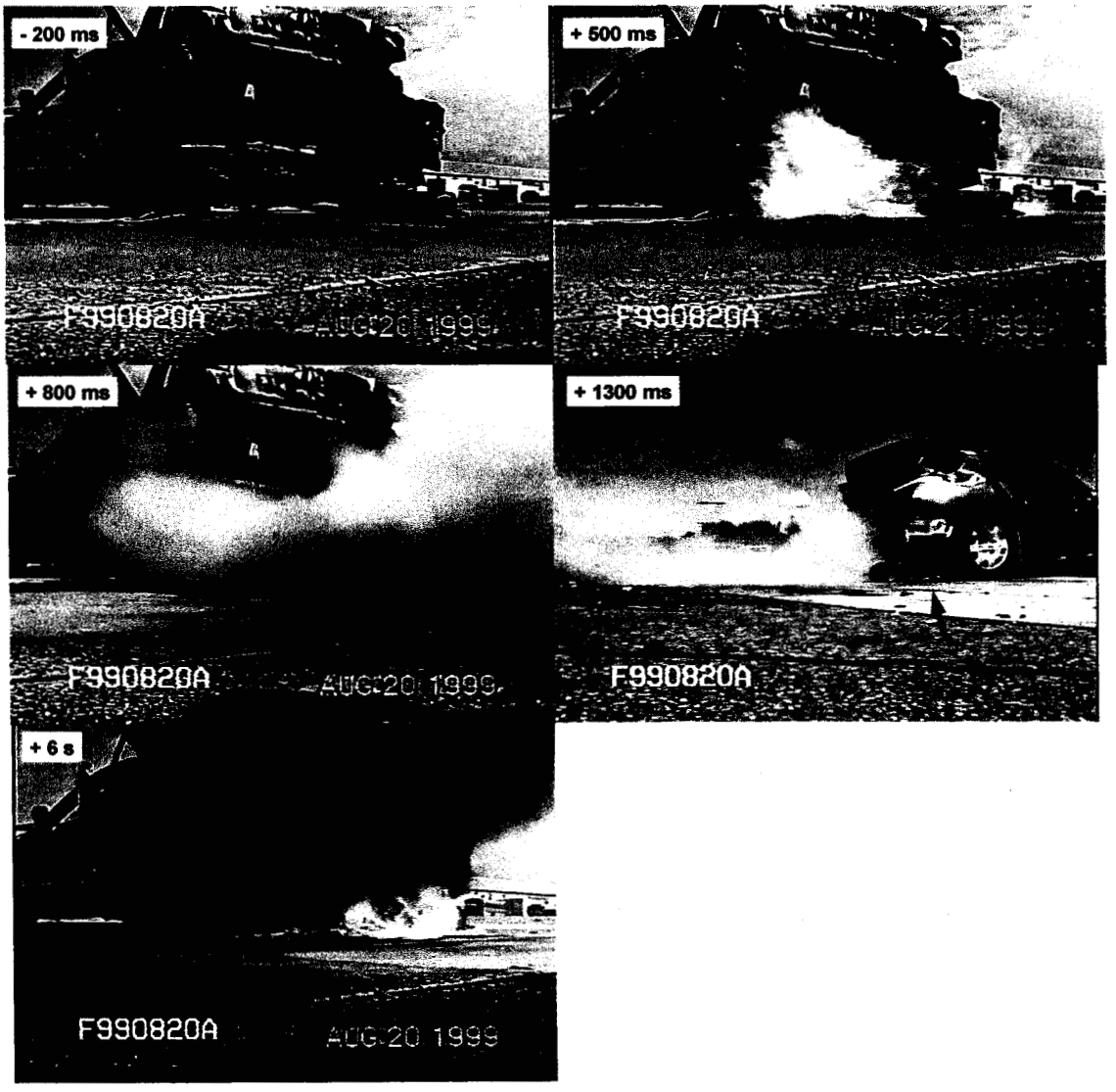

Figure 10. Static Fire Test F990820A. Video stills of this test at 200 ms before ignition (-200 ms), 500 ms after ignition (+ 500 ms), 800 ms after ignition (+ 800 ms), 1300 ms after ignition (+ 1300 ms), and 6 s after ignition (+ 6 s).

3.2.5 Static Test F990820B

The flow rate of gasoline was approximately 3 L/min. Approximately 500 mL of liquid gasoline was poured onto the ground extending about 1000 mm behind the test vehicle. Vapor above liquid gasoline ignited approximately 17.3 s after the start of gasoline flow onto the ground under

the test vehicle. Figure 11 shows plots of the output signals from Detector 1 and Detector 2 to the fire suppression system controller, and the fire pulse from the fire suppression system controller to the SPGG units during this test.

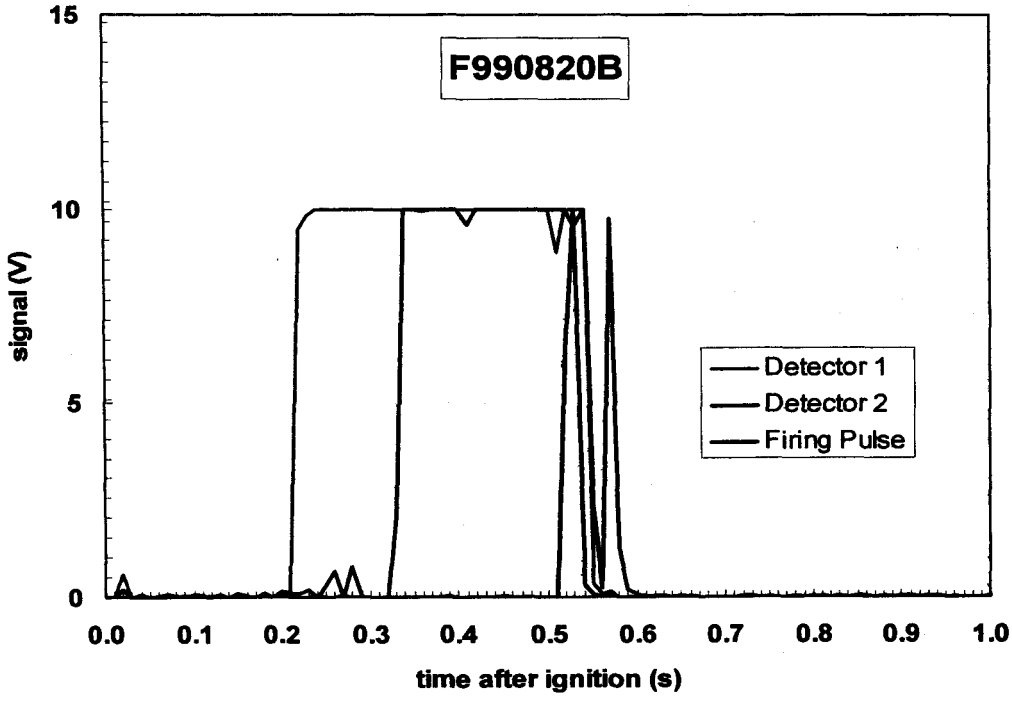

Figure 11. Static Fire Test F990820B. Plots of the output signals from Detectors 1 and 2 to the fire suppression system controller and the firing pulse from the fire suppression system controller to the SPGG units.

Detector 1 output a detection signal to the fire suppression system controller approximately 220 ms after ignition. Detector 2 output a detection signal to the fire suppression system controller approximately 320 ms after ignition. The fire suppression system controller output a firing pulse to the SPGG units approximately 530 ms after ignition. Figure 12 shows a sequence of video stills from this test at 200 ms before ignition, 300 ms after ignition, 600 ms after ignition, and 5 s after ignition. This series of video stills shows that the effluent from the SPGG units extinguished the flames without re-ignition.

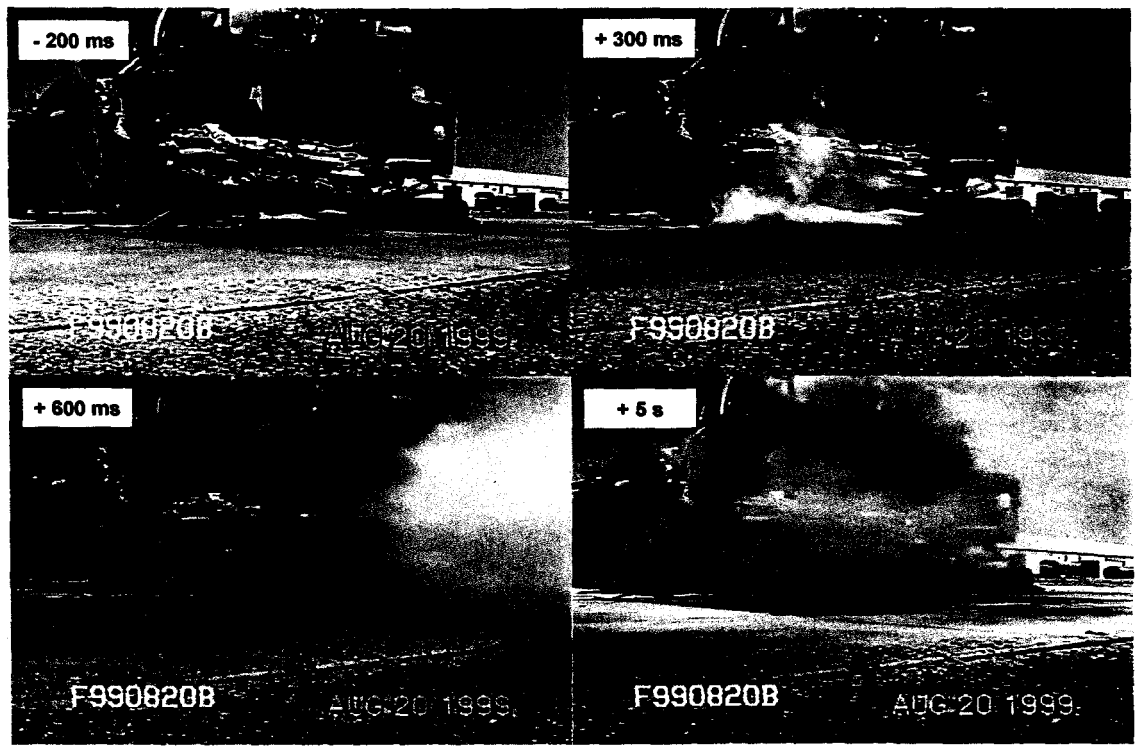

Figure 12. Static Fire Test F990820B. Video stills of this test at 200 ms before ignition (- 200 ms), 300 ms after ignition (+ 300 ms), 600 ms after ignition (+ 600 ms), 5 seconds after ignition (+ 5 s).

3.2.6 Static Test F990820C

The flow rate of gasoline was approximately 3 L/min. Approximately 1000 mL of liquid gasoline was poured onto the ground extending about 2000 mm behind the test vehicle. Vapor above liquid gasoline ignited approximately 38.7 s after the start of gasoline flow onto the ground under the test vehicle. Figure 13 shows plots of the output signals from Detector 1 and Detector 2 to the fire suppression system controller, and the fire pulse from the fire suppression system controller to the SPGG units during this test.

Detector 1 did not output a detection signal to the fire suppression system during this test. Detector 2 output a detection signal to the fire suppression system controller approximately 130 ms after ignition. The fire suppression system controller output firing pulse to the SPGG units approximately 430 ms after ignition.

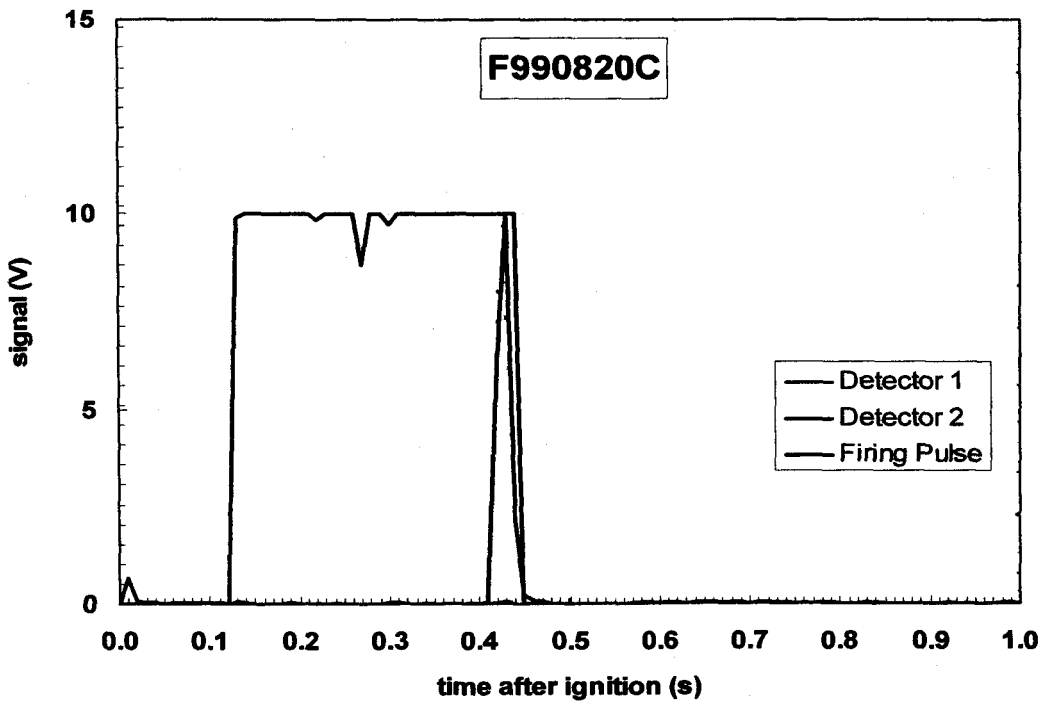

Figure 13. Static Fire Test F990820C. Plots of the output signals from Detectors 1 and 2 to the fire suppression system controller and the firing pulse from the fire suppression system controller to the SPGG units.

Figure 14 shows a sequence of video stills from this test at 200 ms before ignition, 700 ms after ignition, 900 ms after ignition, 2500 ms after ignition, 4830 ms after ignition, and 9 s after ignition. This sequence of video stills shows that the discharge from the SPGG units initially appeared to extinguish the fire. Vapor above the liquid gasoline re-ignited at about 3 s after the SPGG units discharged. Flames appeared to propagate downward from the underbody of the test vehicle (see Fig 14, +4830 ms), suggesting that the effluent from the SPGG units was not distributed to restricted spaces along the vehicle underbody in sufficient quantity to completely extinguish burning gasoline vapor in this area and unextinguished flame(s) in this space(s) acted as the ignition kernel(s) for re-ignition. This is consistent with the experimental set-up in these tests where the outlet of the tube from the external gasoline reservoir was located at the top of the fuel tank. Once gasoline flow was started, liquid gasoline flowed down along the upper surfaces of the fuel tank and dripped from the fuel tank cradle onto the ground under the test vehicle. The flow of gasoline was maintained after activation of the fire suppression system and was a source of gasoline vapor in the space between the top of the fuel tank and the floor panel.

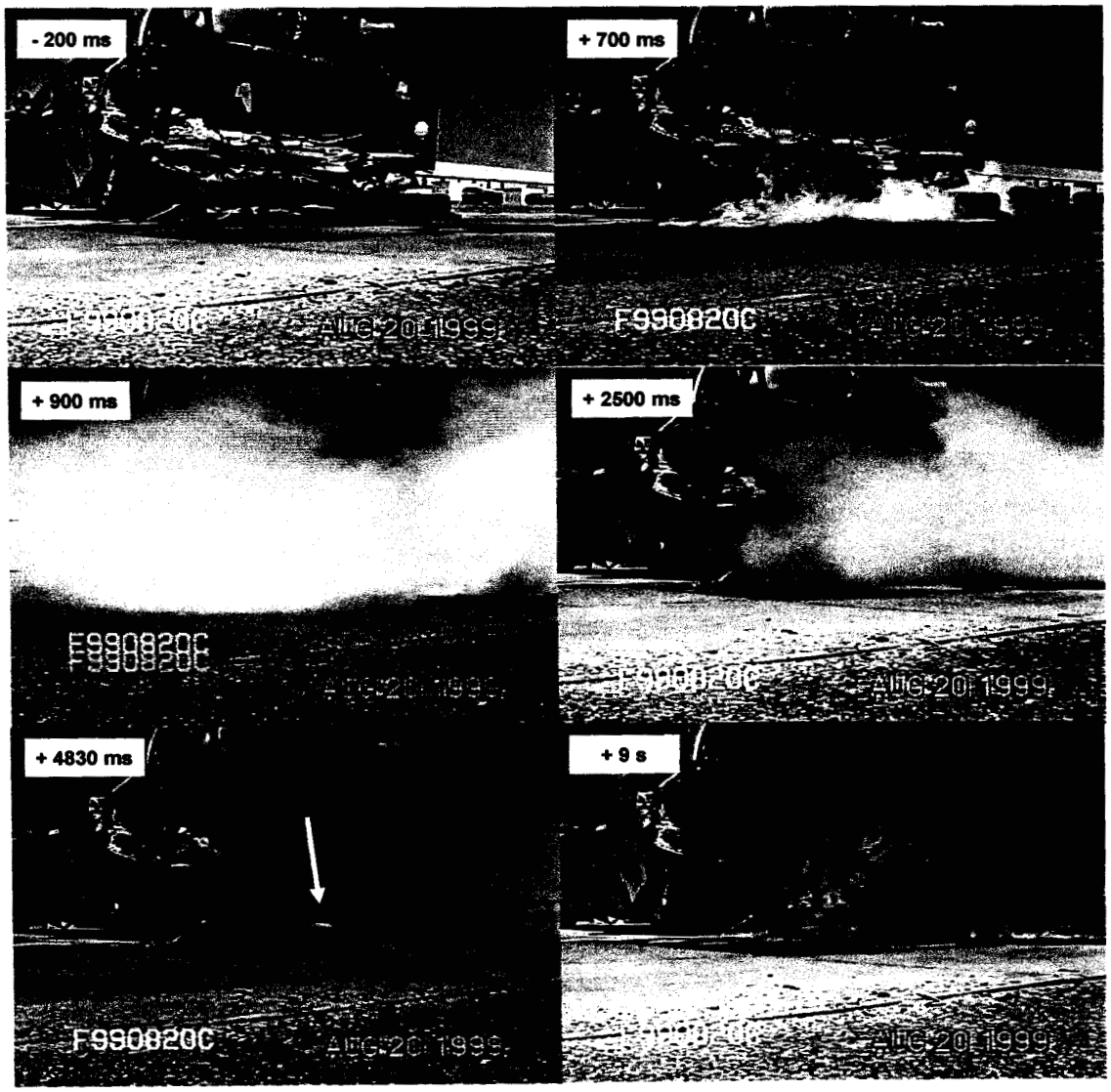

Figure 14. Fire Test F990820C. Video stills of this test at 200 ms before ignition (-200 ms), 700 ms after ignition (+ 700 ms), 900 ms after ignition (+ 900 ms), 2500 ms after ignition (+ 2500 ms), 4830 ms after ignition (+ 4830 ms), and 9 s after ignition (+ 9 s).

4 Summary and Conclusion

A prototype fire suppression system was installed in a test vehicle, and the test vehicle was subjected to a crash test and six static fire tests. The crash test used here was a repeat of a previous crash test that had resulted in a fuel leak. No fuel leak and no fire occurred in the crash test conducted for the study described in this report (C12611). The optical fire detectors and solid-propellant gas generator fire suppressors were operational after this crash test.

A series of six static fire tests of this prototype fire suppression system in the crash tested vehicle were conducted after this crash test. This prototype fire suppression system extinguished the test fires in two of six tests – Static Fire Tests F990819B and F990820B. This prototype fire suppression system failed to extinguish the test fires in four of six tests – Static Fire Tests F990819A, F990819C, F990820A, and F990820C. The batteries that supplied power to the fire suppression system did not have sufficient charge to operate the system in Static Fire Test F990819A. In Static Fire Tests F990819C, F990820A, and F990820C Parts of the crash-tested vehicle shielded sections of the test fires from the SPGG effluent, allowing small areas of gasoline vapor to continue to burn after the SPGG effluent had cleared from the under the test vehicle. These un-extinguished flames re-ignited gasoline under the test vehicle.

The results of the static fire tests described in this report differ markedly from results of testing reported by NIST [2], which suggested that fire suppression systems based on optical detectors and solid propellant gas generators may be effective in suppressing fires involving gasoline spills. The tests conducted by NIST involved evaluation of fire suppression systems based on Halon replacement gaseous agents, dry powder agents, and Solid Propellant Gas Generators. These systems were tested in laboratory tests using engine compartment mock-ups or in the engine compartment of a stationary vehicle with no crash damage. These tests did not simulate real-world dynamic events such as vehicle motion, vehicle crush, or airflow through the engine compartment that occur during a vehicle crash and affect the concentration and distribution of agent within the engine compartment. Moreover, the NIST tests did not allow for substantial accumulation of liquid gasoline on the ground under the test vehicle or for flames extending beyond a well-defined enclosed space. These factors appear to explain the differences between the results of the tests conducted by NIST [2] and the tests described in this report.

References

1. Jack L. Jensen and Jeffrey Santrock. Evaluation of Motor Vehicle Fire Initiation and Propagation. Part 11: Crash Tests on a Front-Wheel Drive Passenger Vehicle. Submitted to the National Highway Transportation Safety Administration pursuant to the Settlement Agreement between General Motors and the Department of Transportation. Submitted May 7, 2002.

2. Anthony Hammins. Evaluation of Active Suppression in Simulated Post-Collision Vehicle Fires. Submitted to the National Highway Transportation Safety Administration pursuant to the Settlement Agreement between General Motors and the Department of Transportation. Submitted March 7, 2001.

3. Hodges, S.E. and Simpson, G. D., "Effective Technologies for Fire Sensing and Suppression on Transit Vehicles," American Public Transportation Association (APTA), Bus Operations and Technologies Conference, May 1995

4. Chattaway, A. C., et al, "The Evaluation of Non-Pyrotechnically Generated Aerosols as Fire Suppressants," Halon Options Technical Working Group (HOTWC), Albuquerque, April 1995.

5. Fire Protection Handbook, "Quantity and Rate of Application of Dry Chemical," p. 6-346, 18th Edition, National fire Protection Association, Quincy, MA, 1997.

6. Vehicle and Mobile Machinery Fire-Extinguishing Systems, Instruction Manual, Kidde Fire Systems, P/N 83-131005-001, Feb. 2001.

7. Yang, J. C. and W. L. Grosshandler, editors, "SOLID PROPELLANT GAS GENERATORS: PROCEEDINGS OF THE 1995 WORKSHOP," NISTIR 5766, NIST, Gaithersburg, MD, Nov. 1995.

8. An explanation of the Joule-Kelvin effect can be found in most Physical Chemistry texts.

Appendix A

Crash Test C12611

Accelerometer Data

Five tri-axial (longitudinal, lateral, and vertical) accelerometers were mounted to each of the test vehicles in the following locations:

- Right front rocker panel
- Left front rocker panel
- Right Rear Rocker Panel
- Left Rear Rocker Panel
- Rear Underbody Floor pan at Fire Sensor

Figure B1 shows the approximate locations of the accelerometers on the test vehicle

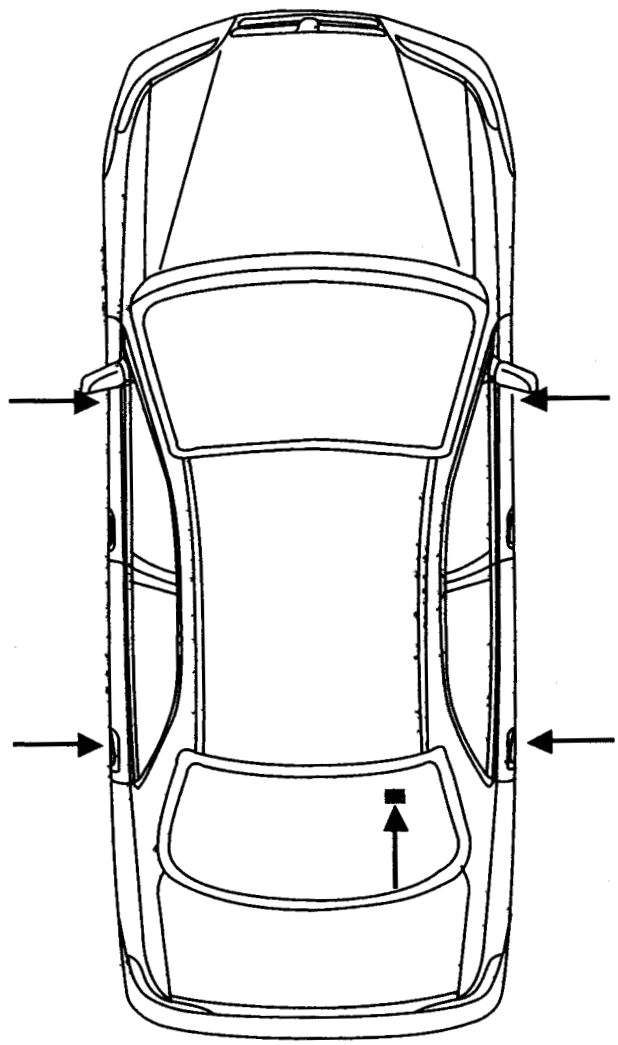

Figure A1. Diagram showing the approximate locations of the accelerometers on the test vehicle.

Two tri-axial (longitudinal, lateral, and vertical) accelerometers were mounted on the Adjustable Moving Deformable Barrier AMDB in the following locations:

- Rear cross member
- Center of Mass

Figure A2 shows the approximate locations of the accelerometers on the Adjustable Moving Deformable Barrier.

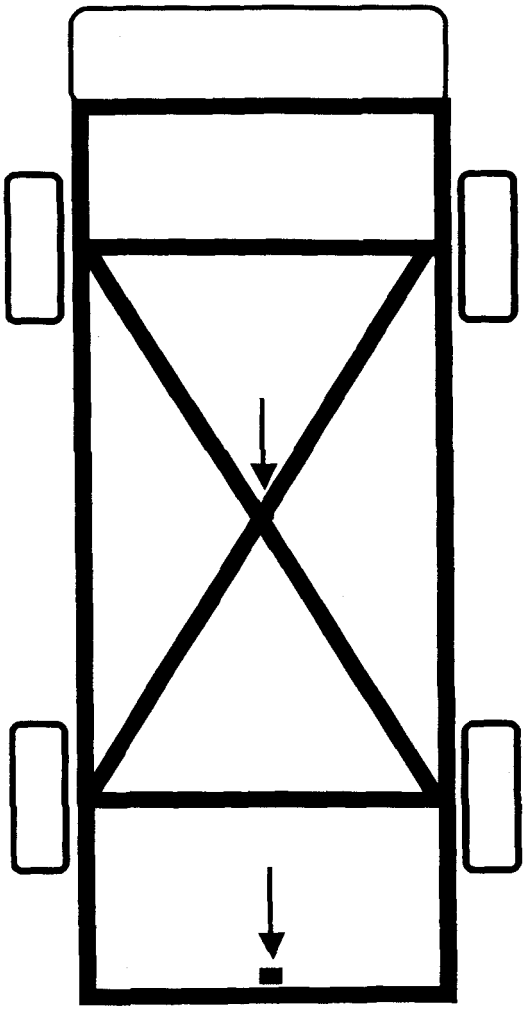

Figure A2. Diagram showing the approximate of the accelerometers on locations Adjustable Moving Deformable Barrier.

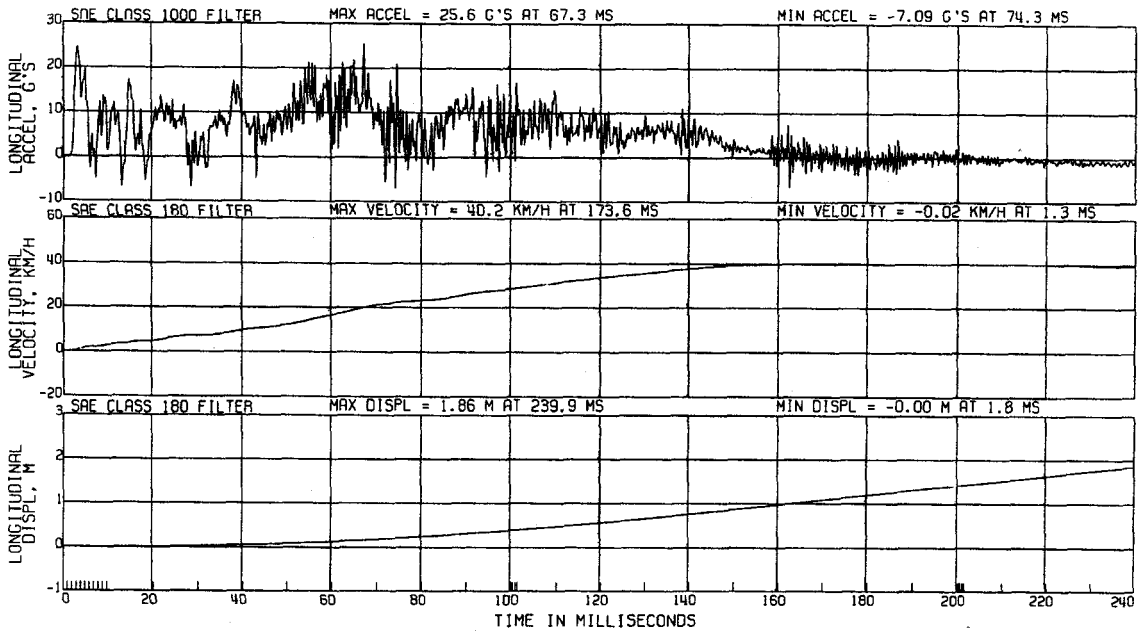

Plot A1. Crash Test C12611. Plots of acceleration, velocity, and displacement in the direction of the longitudinal-axis calculated from the accelerometer on the left front rocker.

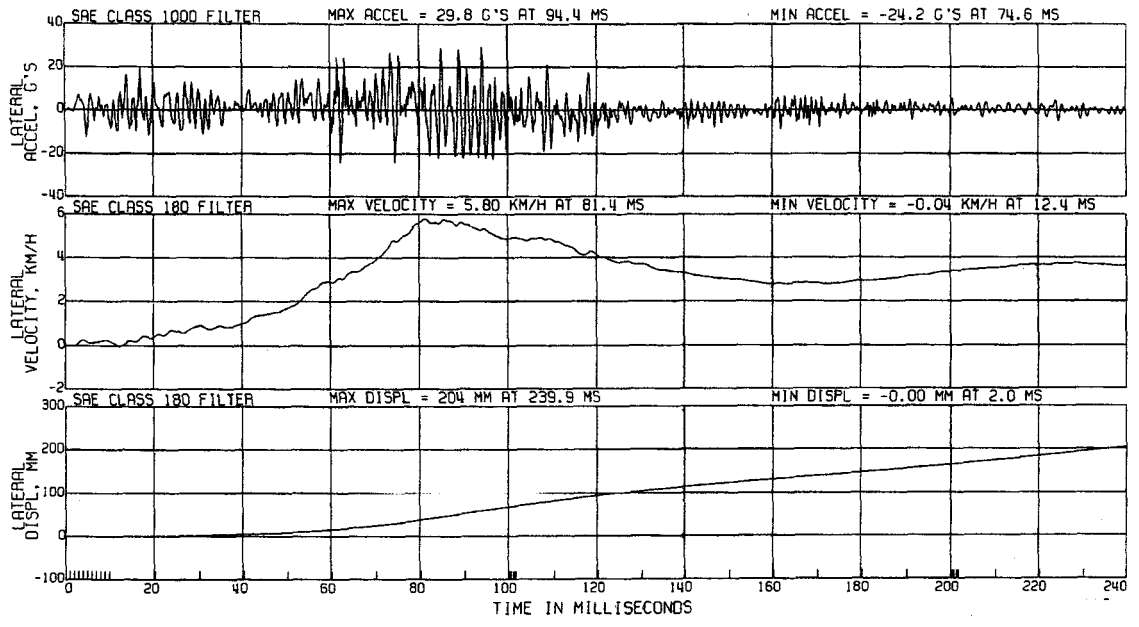

Plot A2. Crash Test C12611. Plots of acceleration, velocity, and displacement in the direction of the lateral-axis calculated from the accelerometer on the left front rocker.

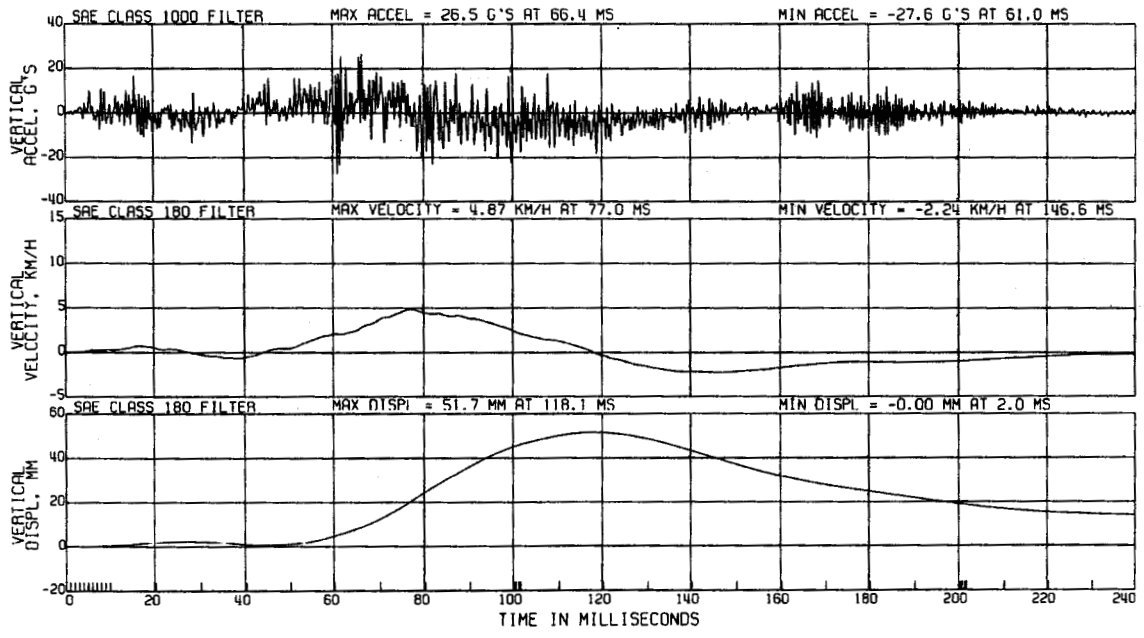

Plot A3. Crash Test C12611. Plots of acceleration, velocity, and displacement in the direction of the vertical-axis calculated from the accelerometer on the left front rocker.

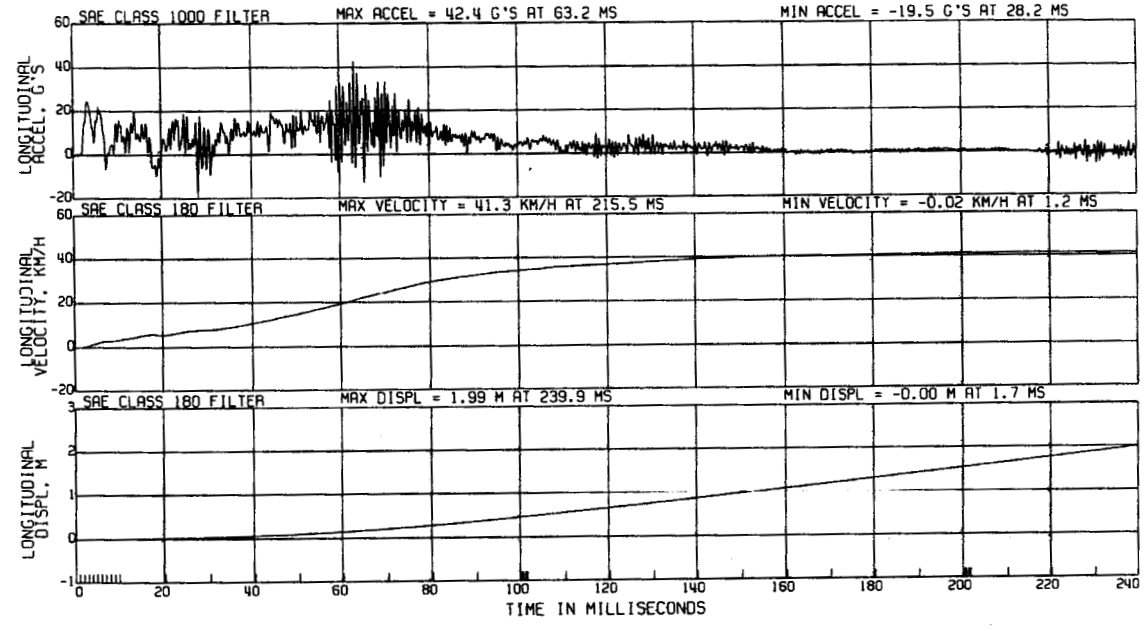

Plot A4. Crash Test C12611. Plots of acceleration, velocity, and displacement in the direction of the longitudinal-axis calculated from the accelerometer on the right front rocker.

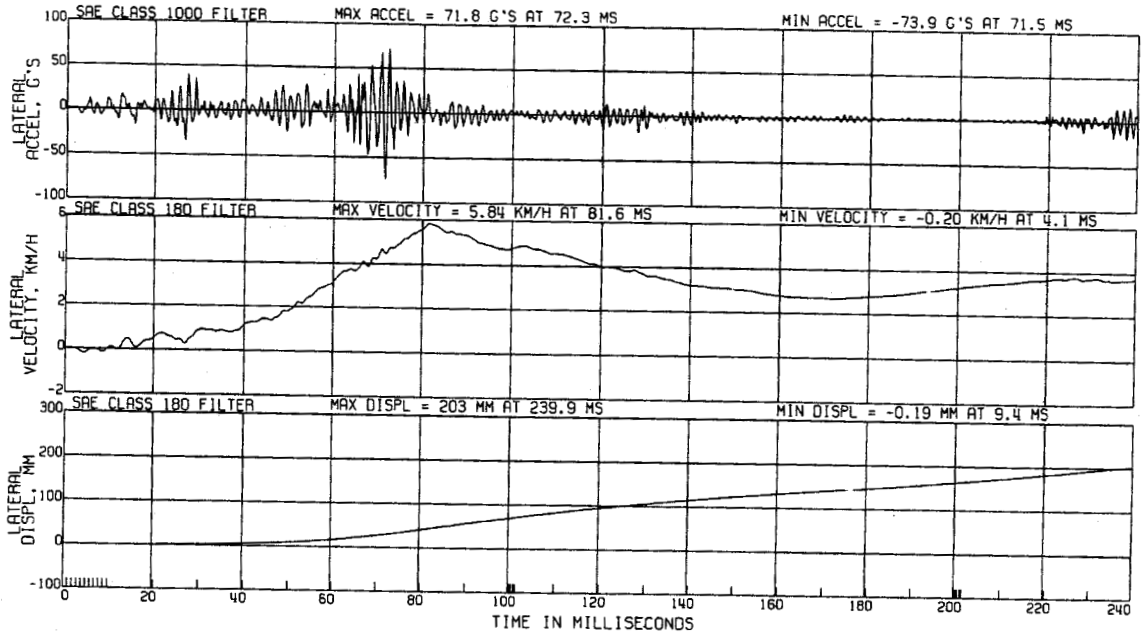

Plot A5. Crash Test C12611. Plots of acceleration, velocity, and displacement in the direction of the lateral-axis calculated from the accelerometer on the right front rocker.

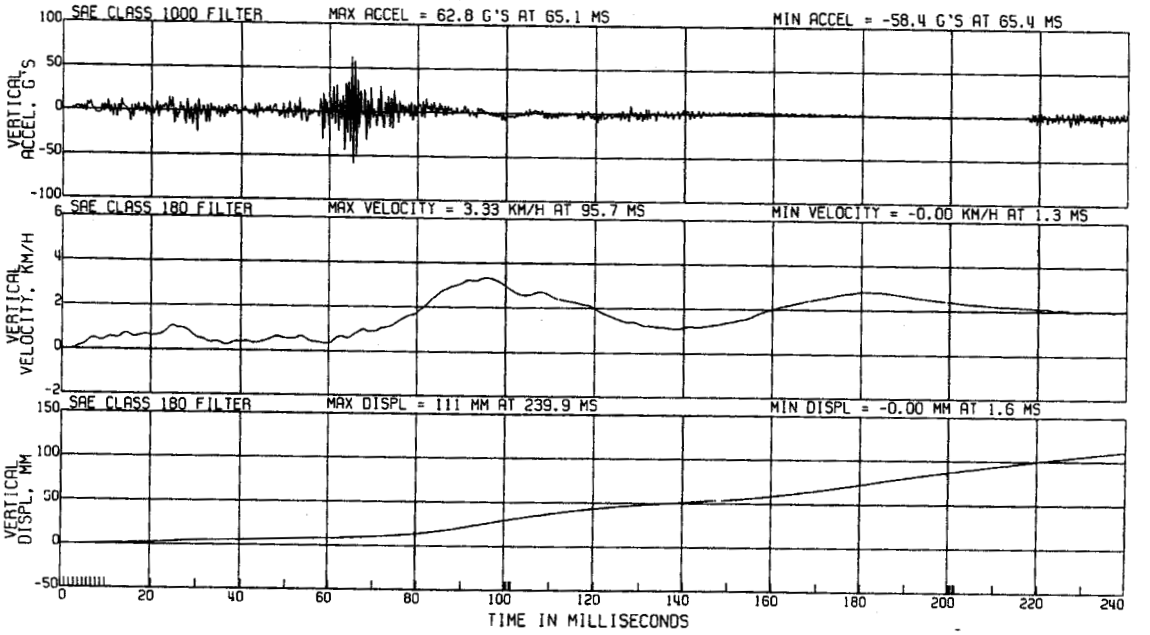

Plot A6. Crash Test C12611. Plots of acceleration, velocity, and displacement in the direction of the vertical-axis calculated from the accelerometer on the right front rocker.

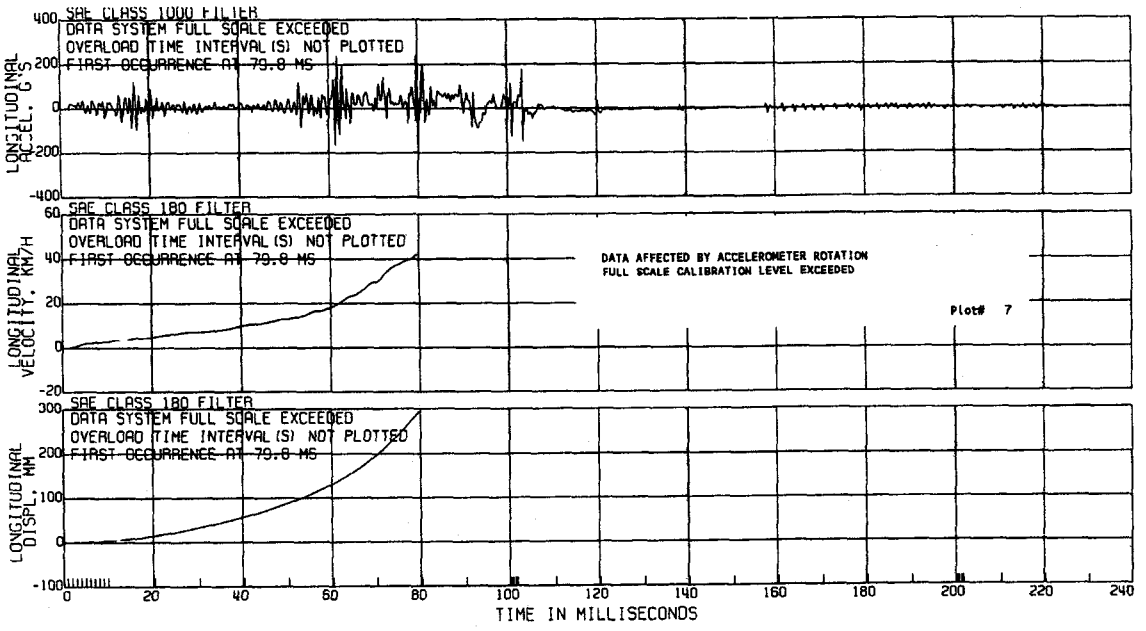

Plot A7. Crash Test C12611. Plots of acceleration, velocity, and displacement in the direction of the longitudinal-axis calculated from the accelerometer on the left rear rocker.

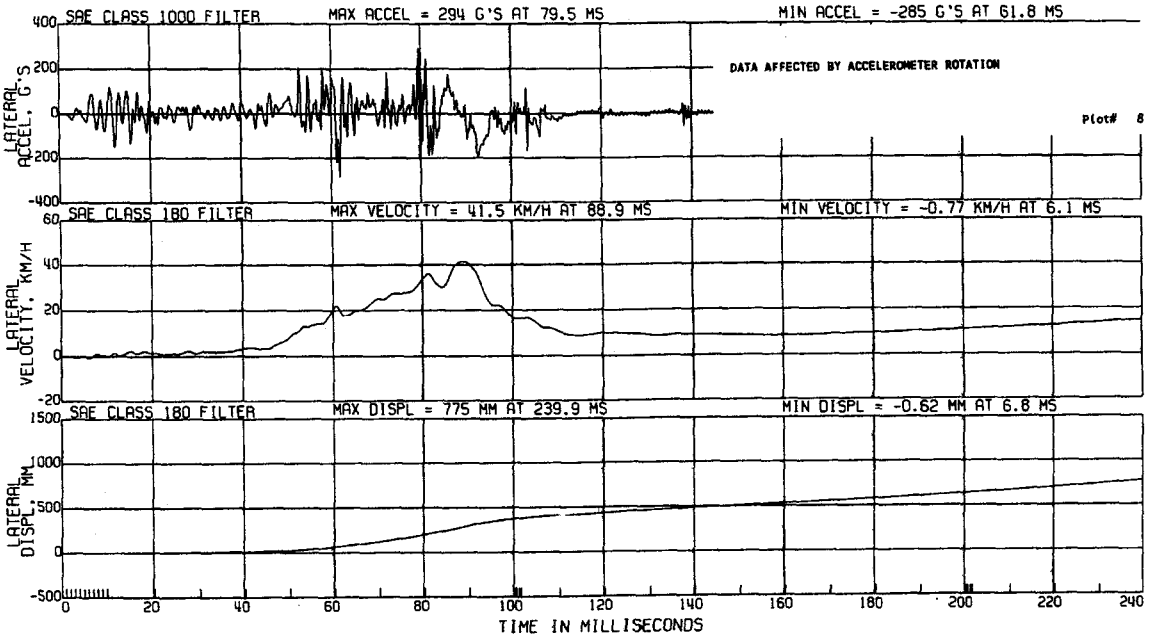

Plot A8. Crash Test C12611. Plots of acceleration, velocity, and displacement in the direction of the lateral-axis calculated from the accelerometer on the left rear rocker.

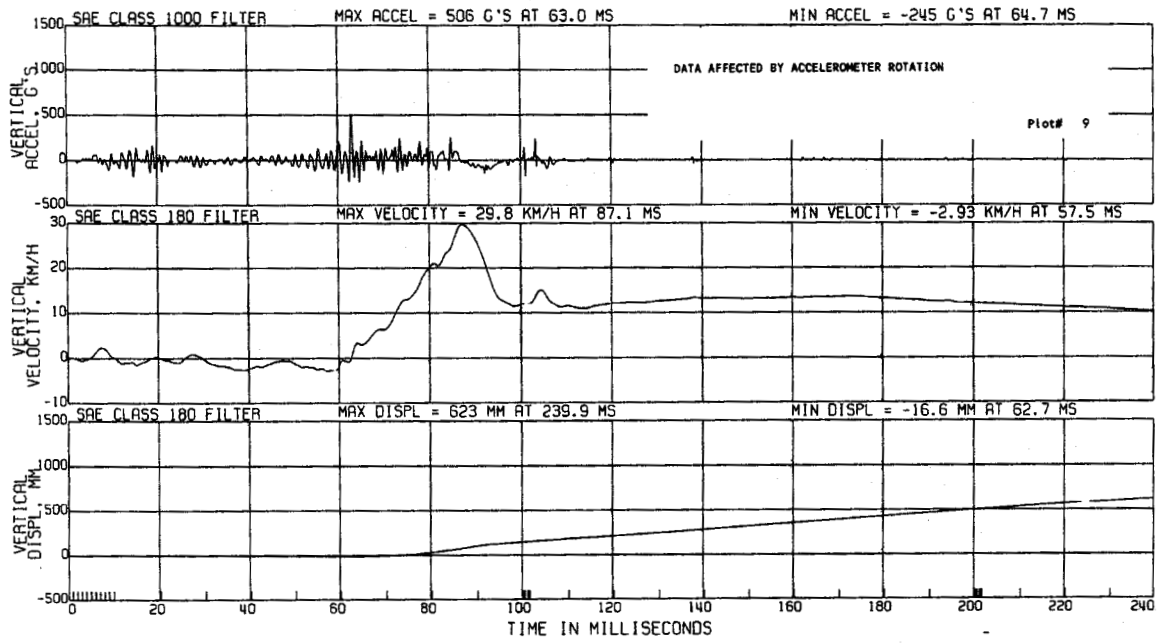

Plot A9. Crash Test C12611. Plots of acceleration, velocity, and displacement in the direction of the vertical-axis calculated from the accelerometer on the left rear rocker.

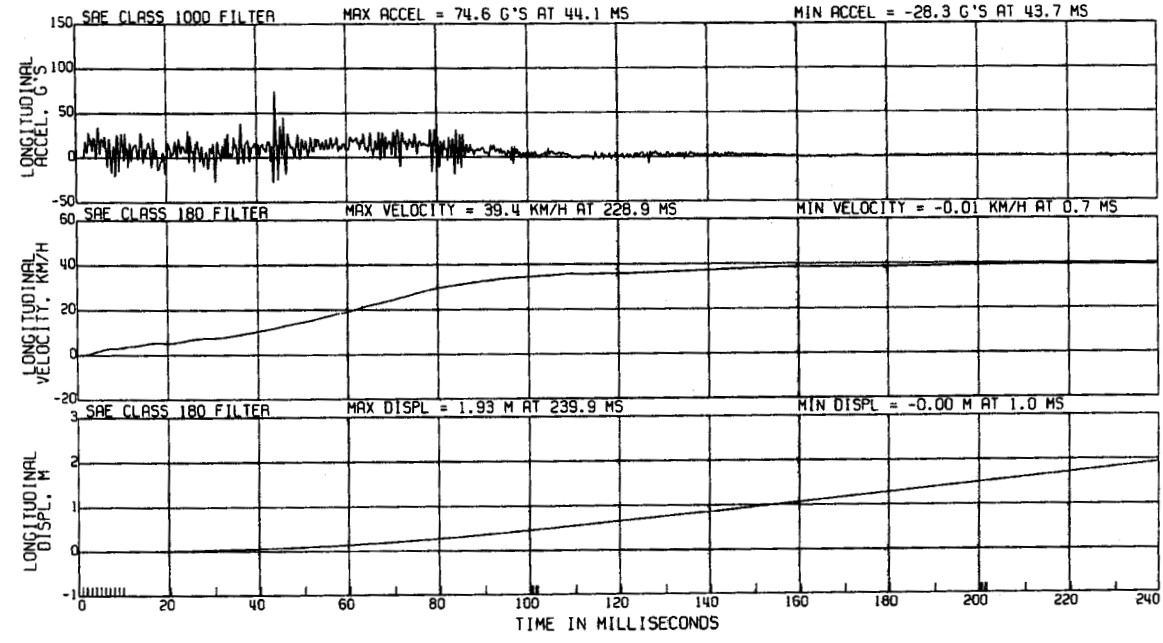

Plot A10. Crash Test C12611. Plots of acceleration, velocity, and displacement in the direction of the longitudinal-axis calculated from the accelerometer on the right rear rocker.

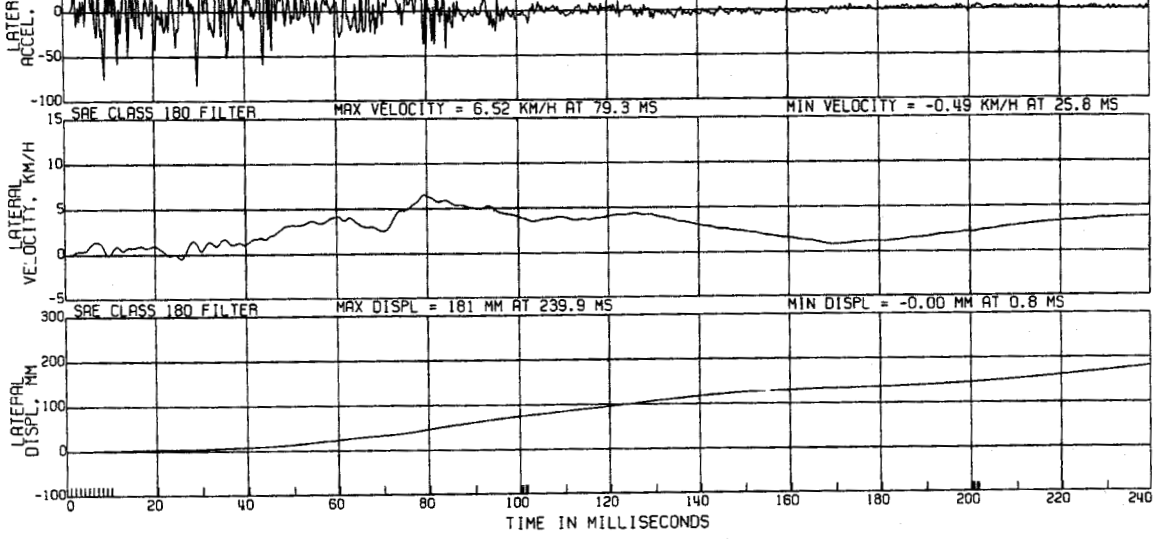

Plot A11. Crash Test C12611. Plots of acceleration, velocity, and displacement in the direction of the lateral-axis calculated from the accelerometer on the right rear rocker.

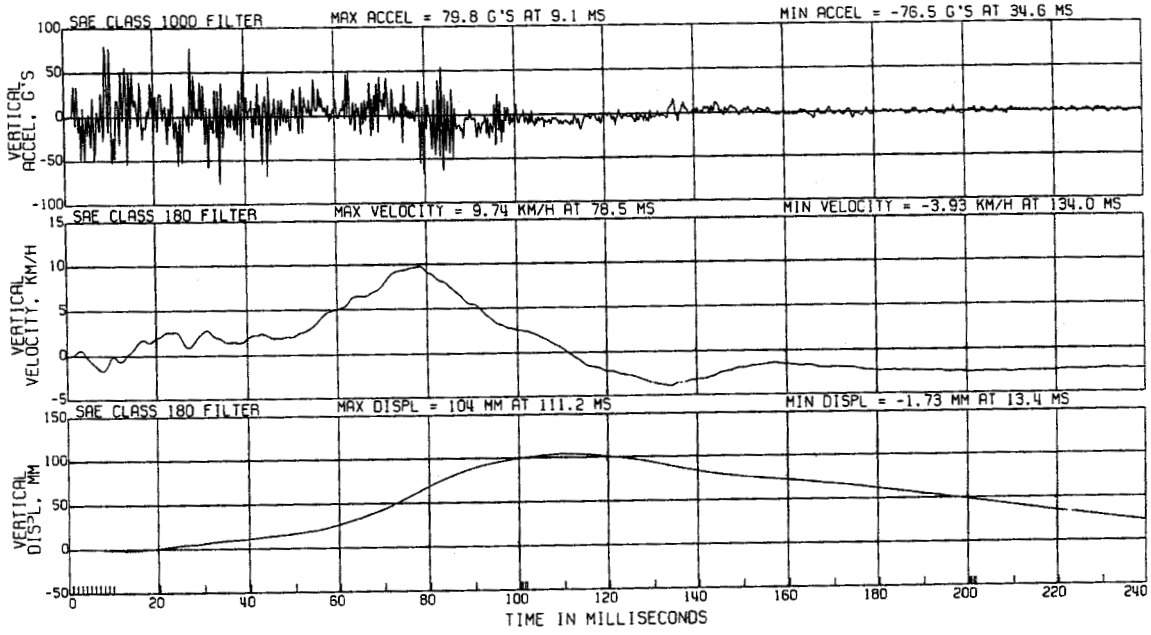

Plot A12. Crash Test C12611. Plots of acceleration, velocity, and displacement in the direction of the vertical-axis calculated from the accelerometer on the right rear rocker

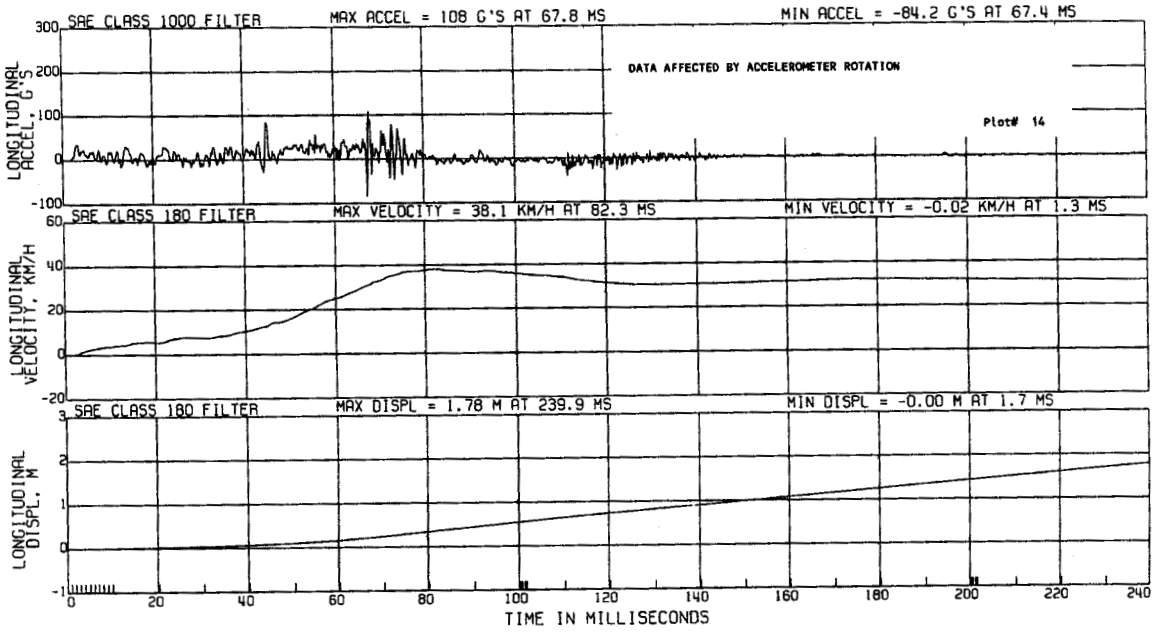

Plot A13. Crash Test C12611. Plots of acceleration, velocity, and displacement in the direction of the longitudinal-axis calculated from the accelerometer on the rear floorpan at the fire sensor.

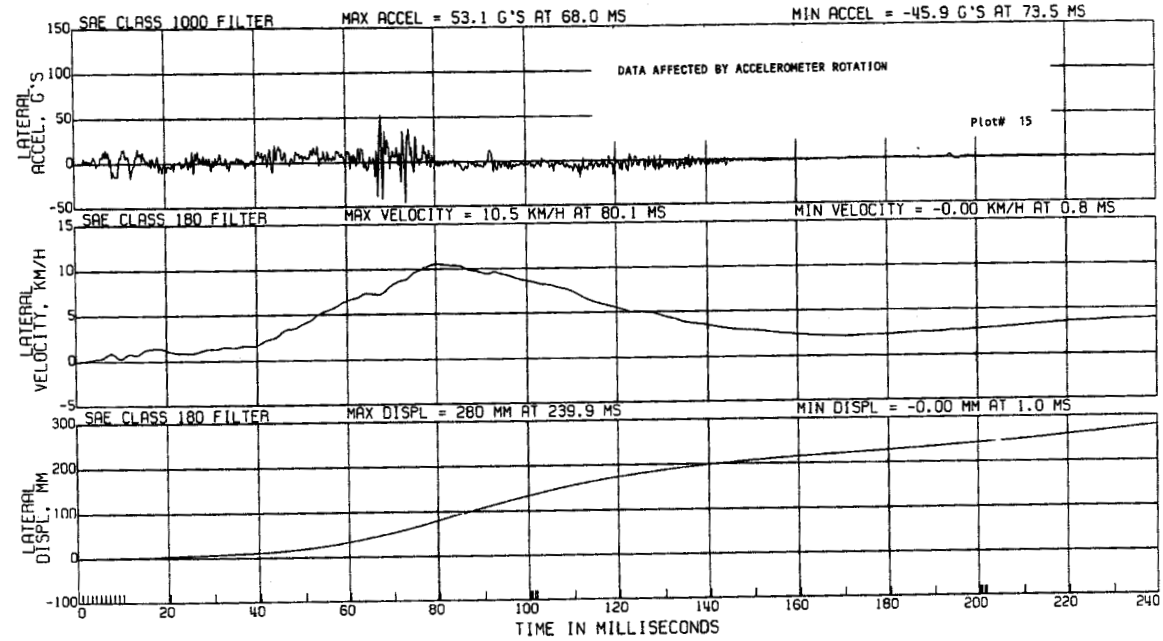

Plot A14. Crash Test C12611. Plots of acceleration, velocity, and displacement in the direction of the lateral-axis calculated from the accelerometer on the rear floorpan at the fire sensor.

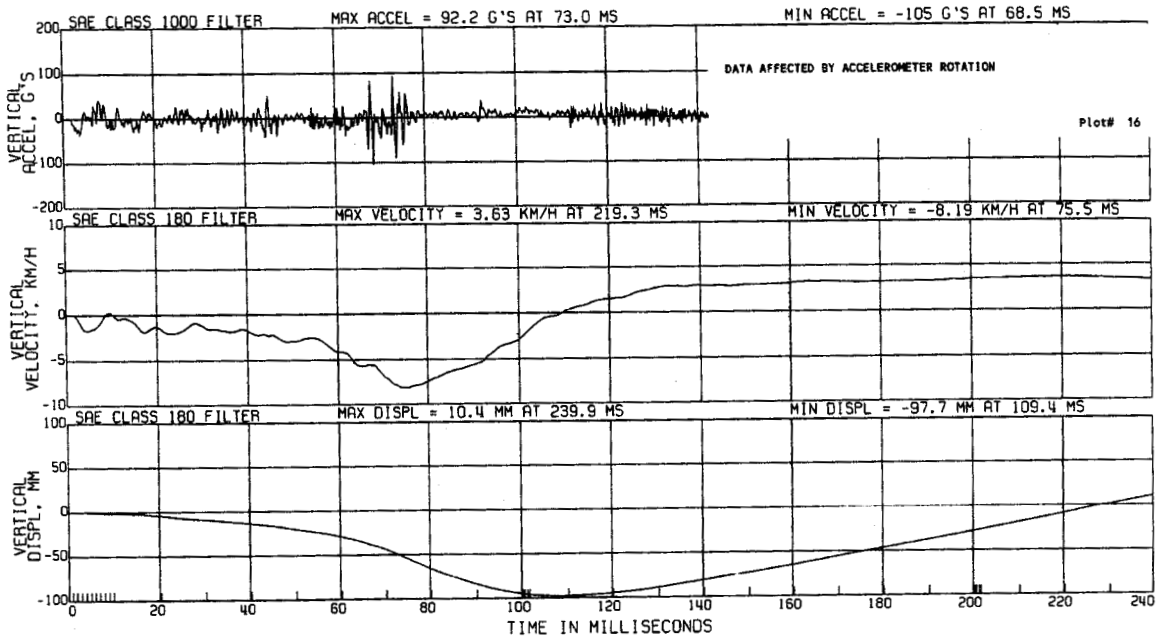

Plot A15. Crash Test C12611. Plots of acceleration, velocity, and displacement in the direction of the vertical-axis calculated from the aocelerometer on the rear floorpan at the fire sensor.

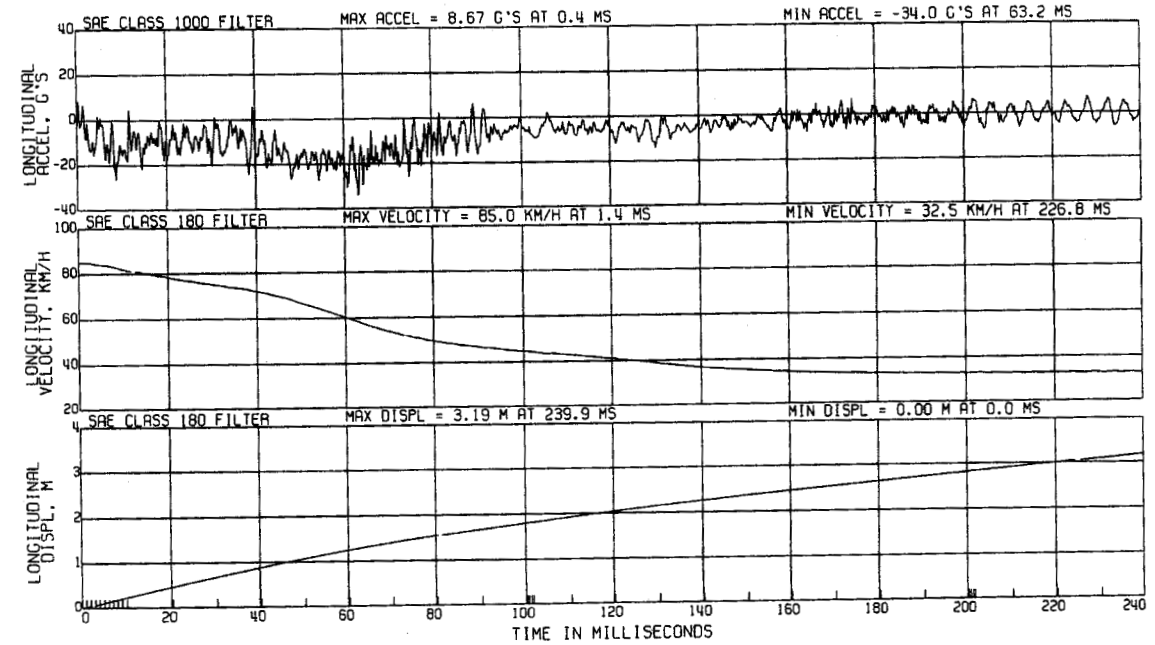

Plot A16. Crash Test C12611. Plots of acceleration, velocity, and displacement in the direction of the longitudinal-axis calculated from the accelerometer at the Center of Mass on the AMDB.

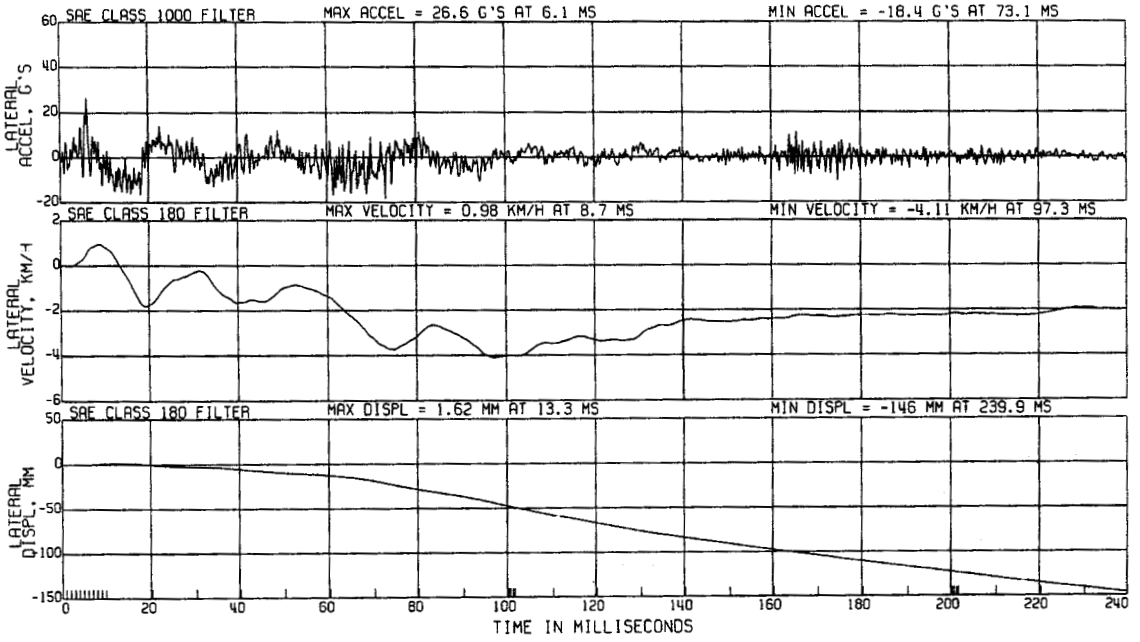

Plot A17. Crash Test C12611. Plots of acceleration, velocity, and displacement in the direction of the lateral-axis calculated from the accelerometer at the Center of Mass on the AMDB.

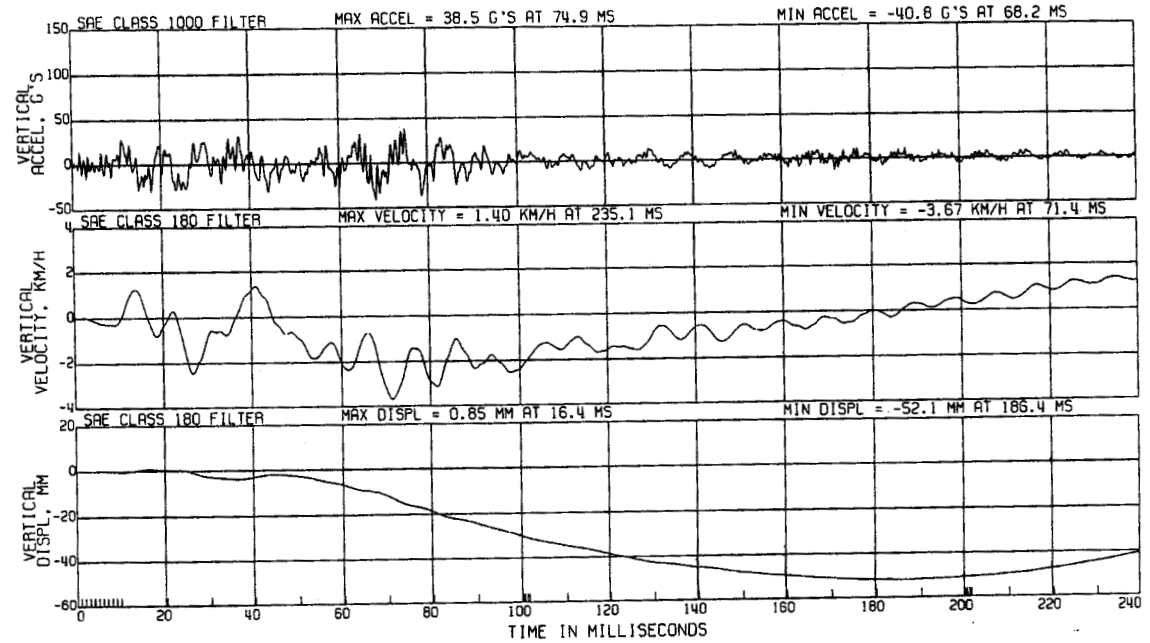

Plot A18. Crash Test C12611. Plots of acceleration, velocity, and displacement in the direction of the vertical-axis calculated from the accelerometer at the Center of Mass on the AMDB.

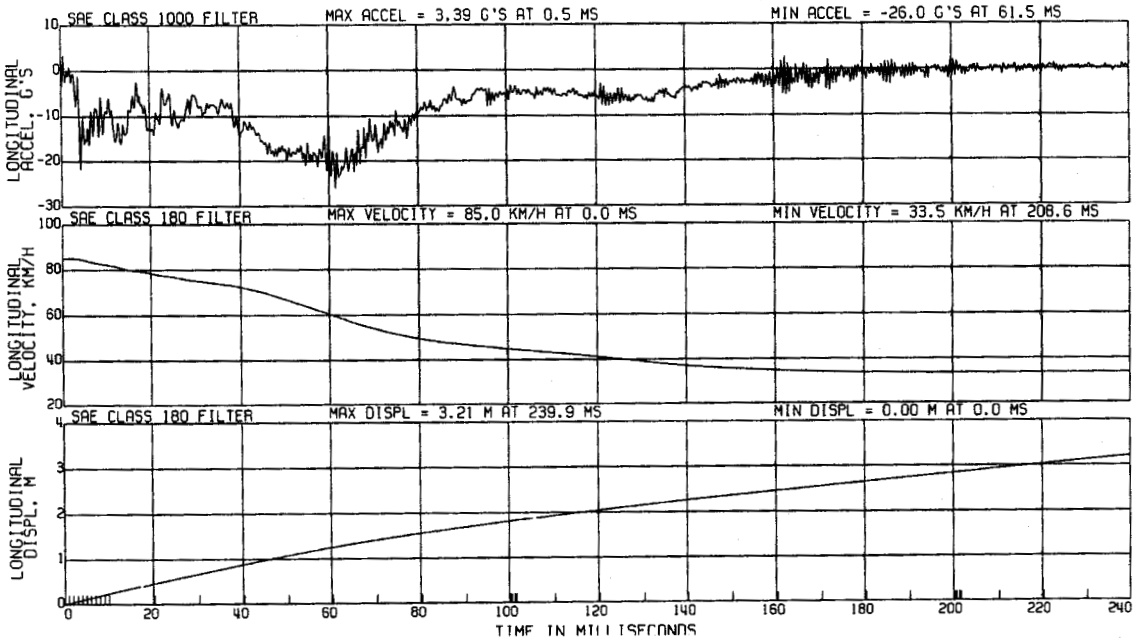

Plot A19. Crash Test C12611. Plots of acceleration, velocity, and displacement in the direction of the longitudinal-axis calculated from the accelerometer on the rear cross member on the AMDB.

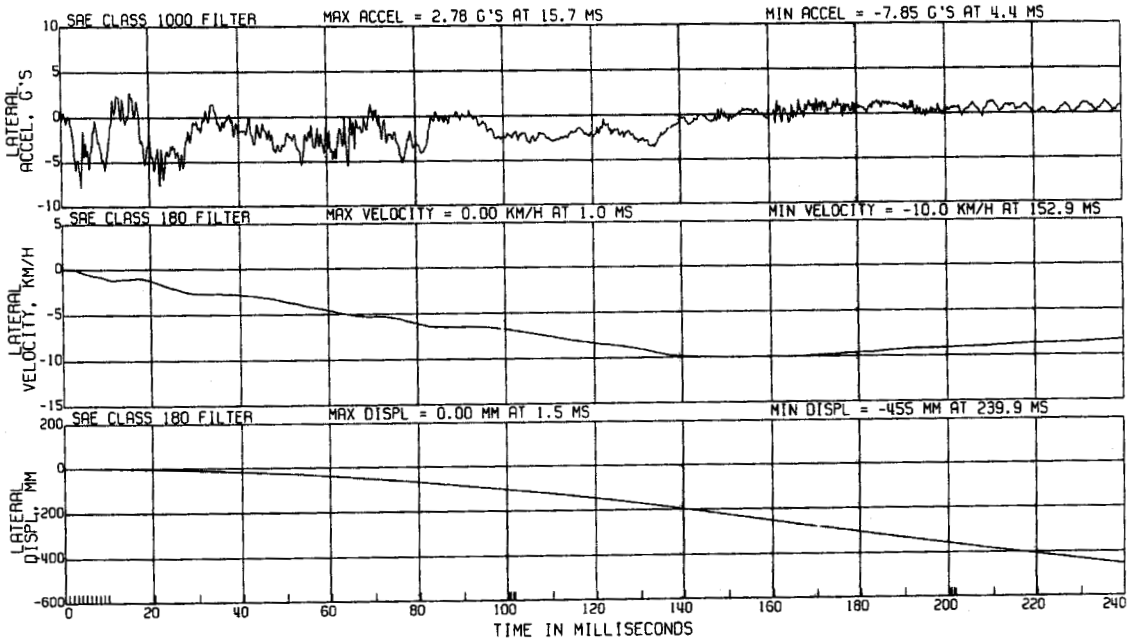

Plot A20. Crash Test C12611. Plots of acceleration, velocity, and displacement in the direction of the lateral-axis calculated from the accelerometer on the rear cross member on the AMDB.

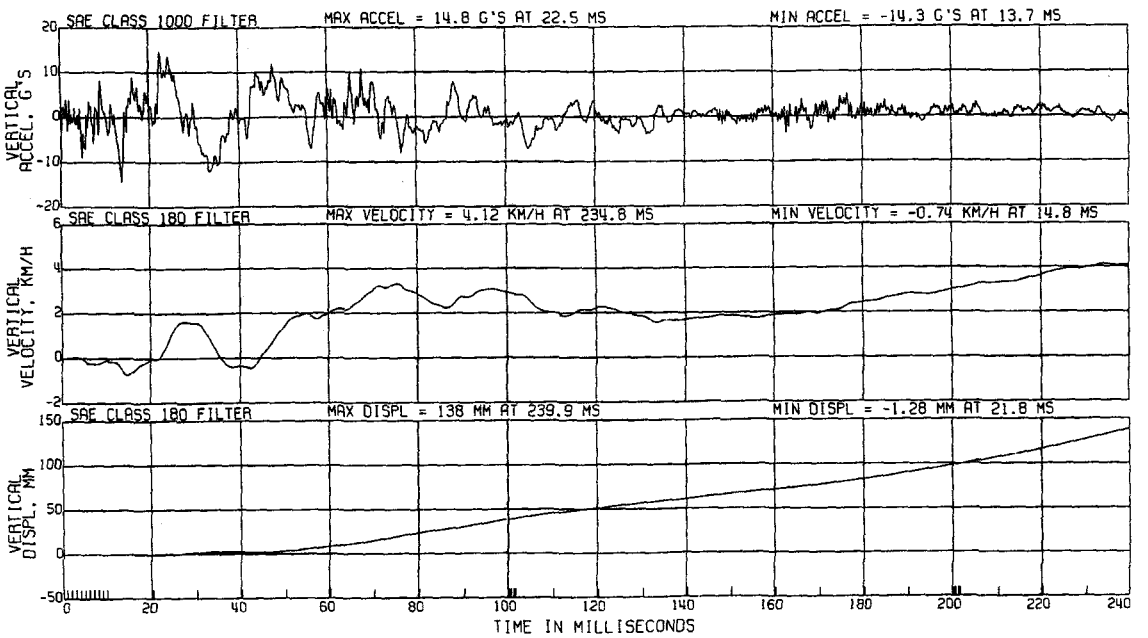

Plot A21. Crash Test C12611. Plots of acceleration, velocity, and displacement in the direction of the vertical-axis calculated from the accelerometer on the rear cross member on the AMDB.

Appendix B

Flammable Vapor Sensor Data

Crash Test C12611

Five flammable gas sensors (TGS 813, FIGARO USA, Inc, Wilmette, IL) were installed in the engine compartments of the test vehicle. Gas Sensor S1 was located at the right side rear cross member in fuel tank cradle. Gas Sensor S2 was located at the center of rear cross member in fuel tank cradle. Gas Sensor S3 was located at the left side rear cross member in fuel tank cradle. Gas Sensor S4 was located at the left side of the front cross member in the fuel tank cradle. Gas Sensor S5 was located above fuel tank and below the trunk floor panel. Figures B1 through B4 show the locations of Sensors S1 through S4 in the test vehicle. Sensor S5 was obscured from view and could not be photographed.

Gas phase concentration – sensor output voltage calibration data was obtained using heptane in the range of 0 to 5% (V/V). Estimates of the flammable gas concentration at each location in the engine compartment of both test vehicles using this calibration data are shown in Plots B1 through B5.

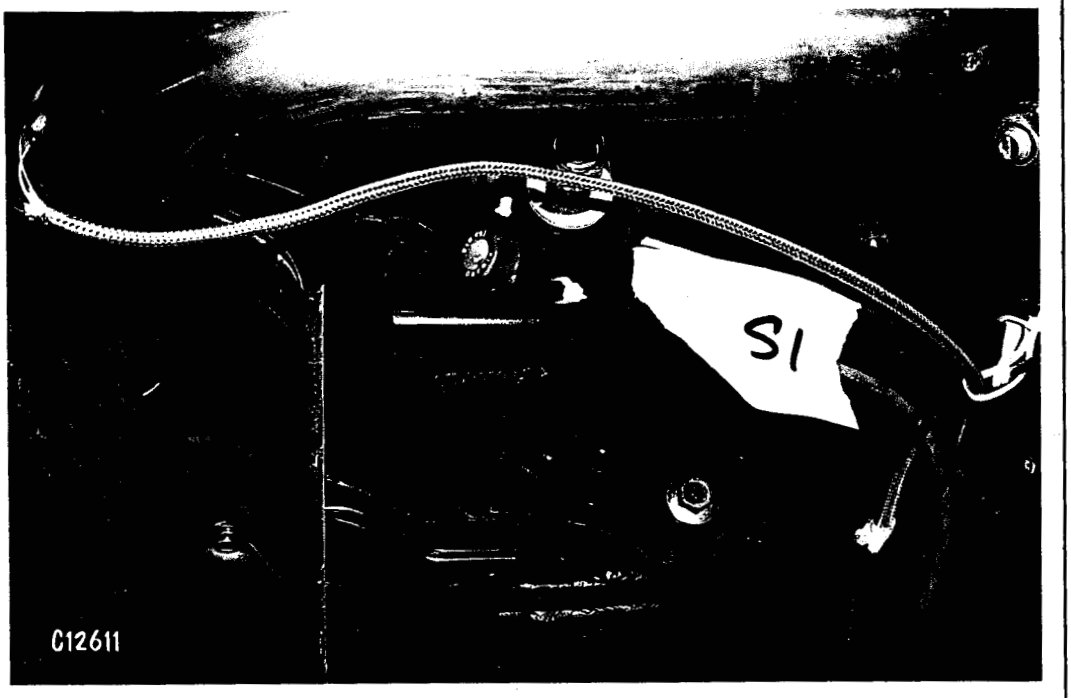

Figure B1. Crash Test C12611. Photograph of the location of flammable gas sensor S1 in test vehicle.

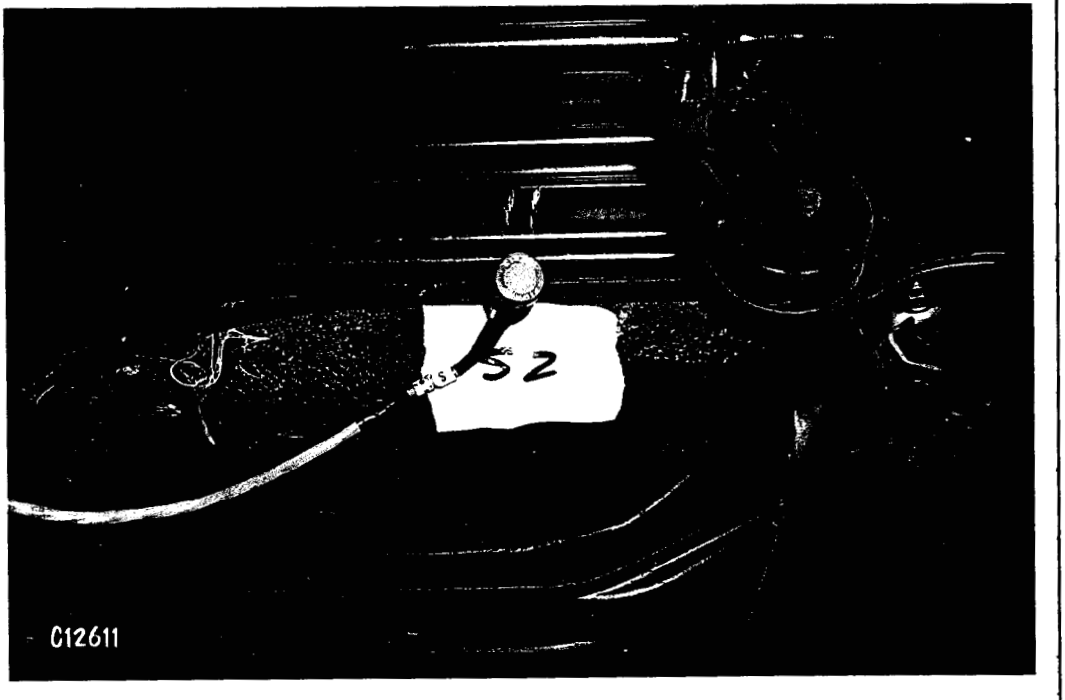

Figure B2. Crash Test C12611. Photograph of the location of flammable gas sensor S2 in test vehicle.

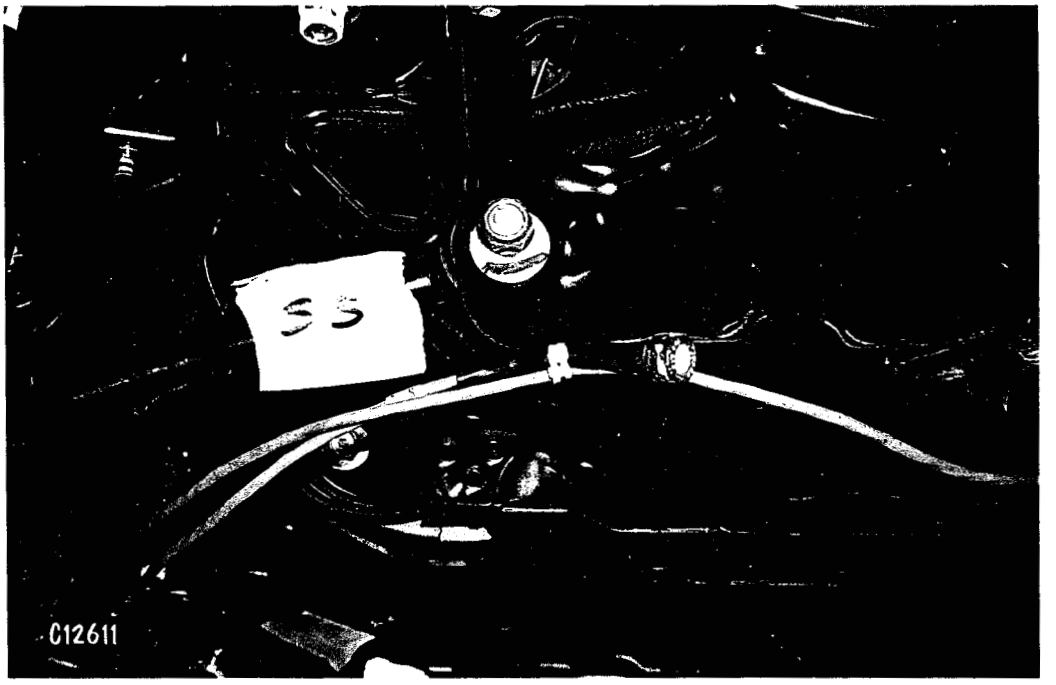

Figure B3. Crash Test C12611. Photograph of the location of flammable gas sensor S3 in test vehicle.

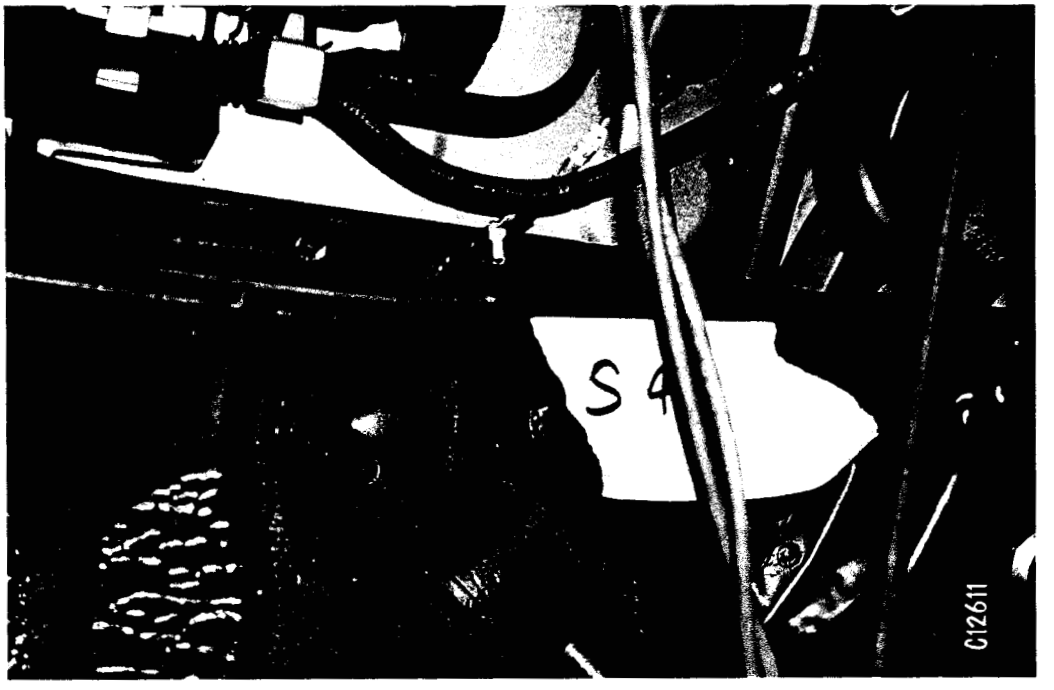

Figure B4. Crash Test C12611. Photograph of the location of flammable gas sensor S4 in test vehicle.

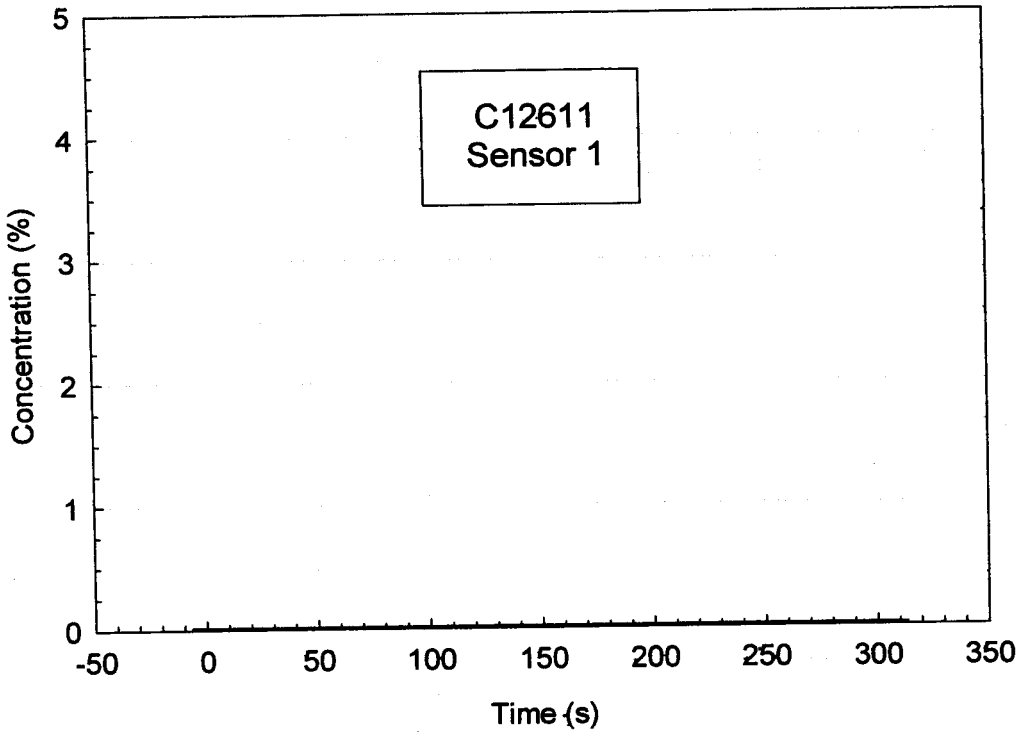

Plot B1. Crash Test C12611. Plot of flammable vapor concentration recorded by the flammable gas sensor at Location 1.

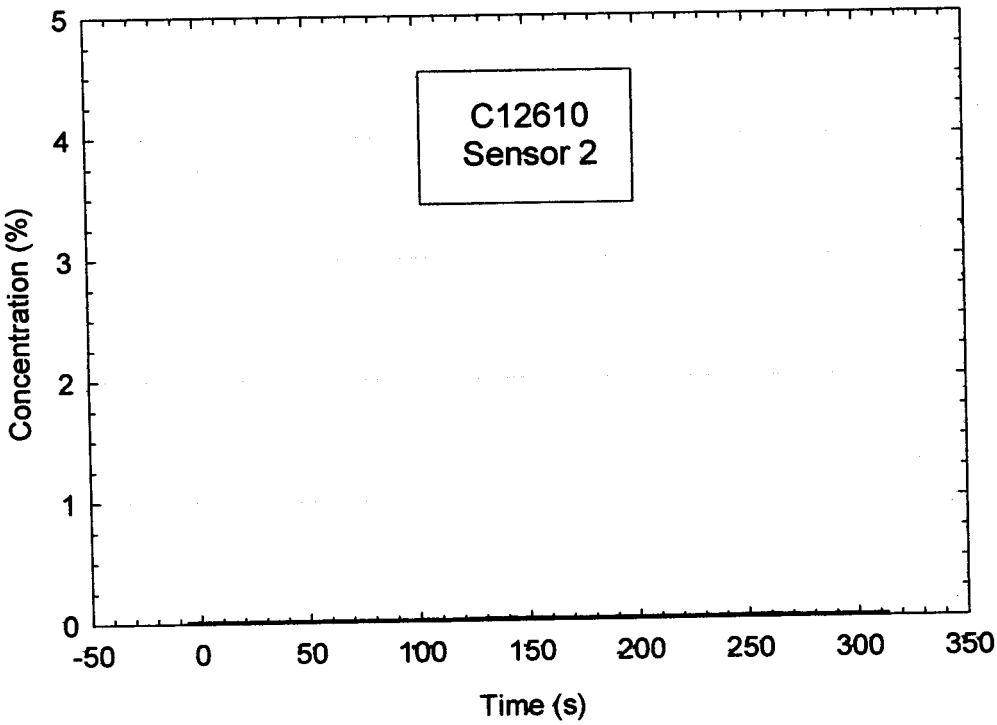

Plot B2. Crash Test C12611. Plot of flammable vapor concentration recorded by the flammable gas sensor at Location 2.

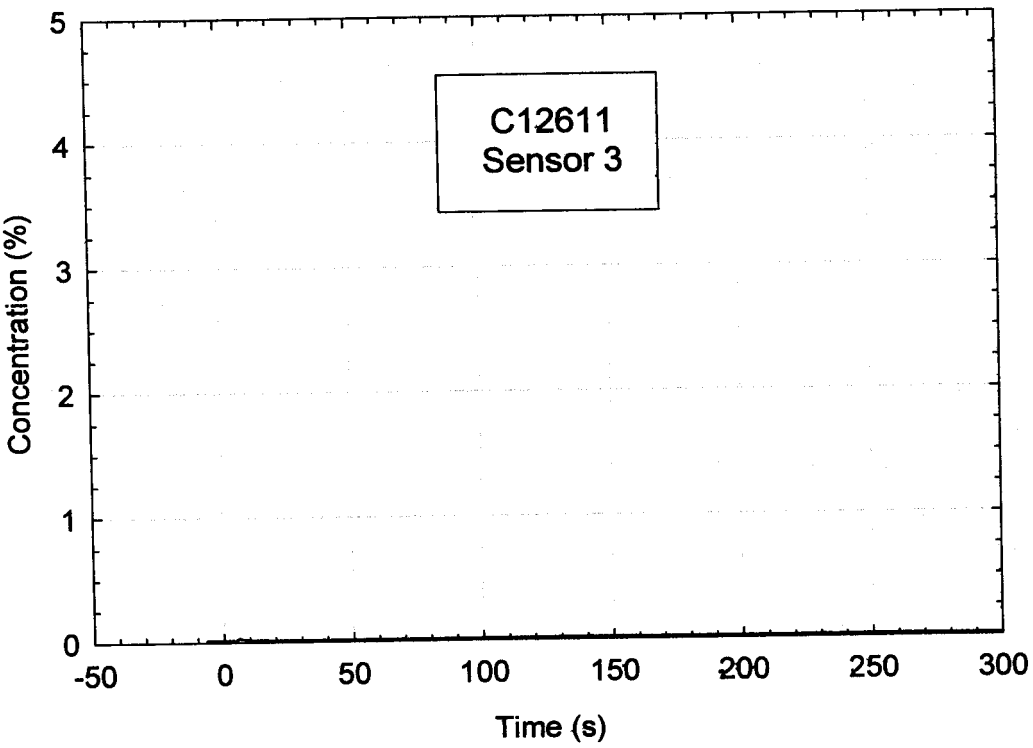

Plot B3. Crash Test C12611. Plot of flammable vapor concentration recorded by the flammable gas sensor at Location 3.

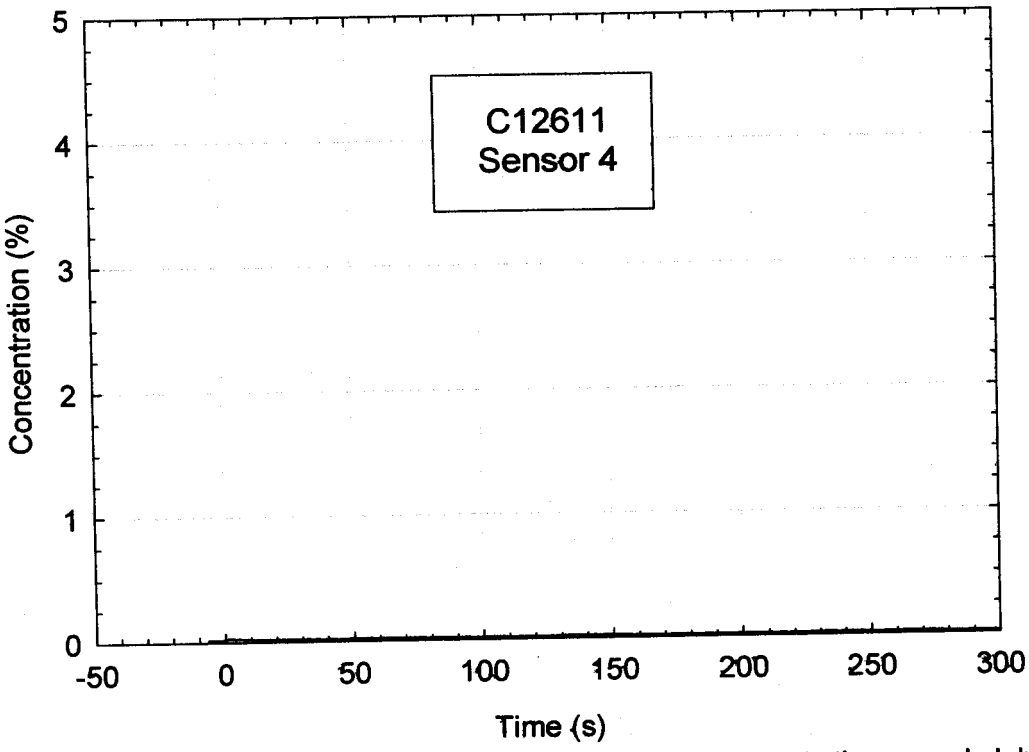

Plot B4. Crash Test C12611. Plot of flammable vapor concentration recorded by the flammable gas sensor at Location 4.

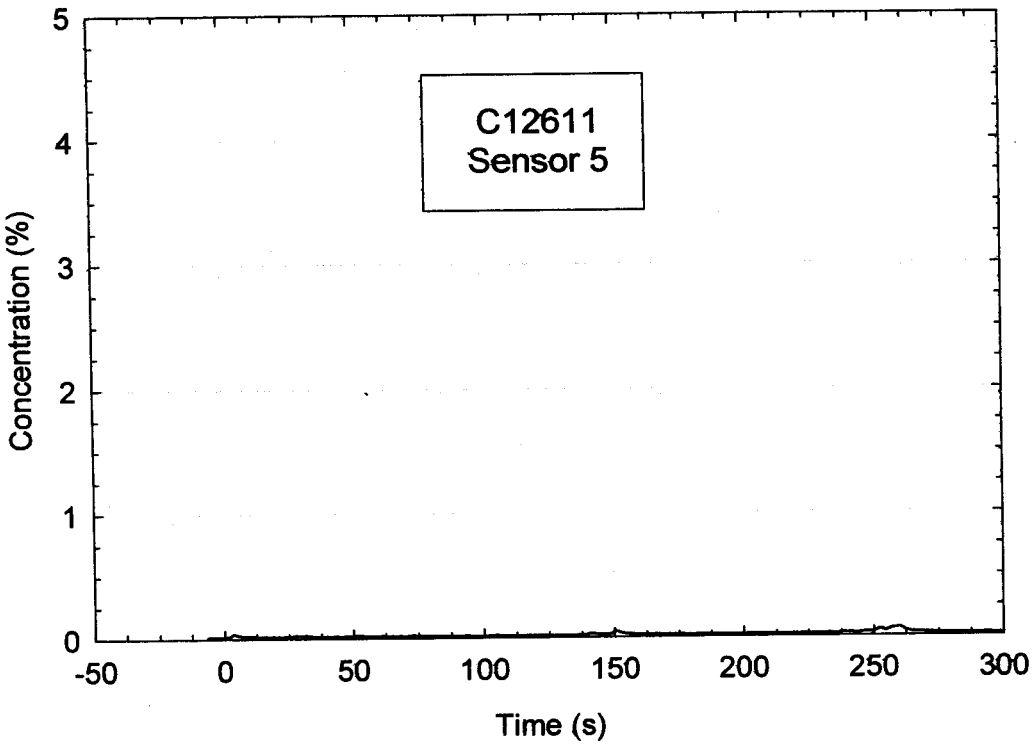

Plot B5. Crash Test C12611. Plot of flammable vapor concentration recorded by the flammable gas sensor at Location 5.

Appendix C

Gas Chromatography / Mass Spectroscopy Data

Crash Test C12611

Appendix D

Component Temperature Data

Crash Test C12611

Five thermocouples were installed in the test vehicle for this crash test. Four thermocouples were intrinsically welded to exhaust system components. One shielded thermocouple was used to measure air temperature near the exhaust system. Figure B3 is a drawing showing the approximate locations of these thermocouples on the test vehicle.

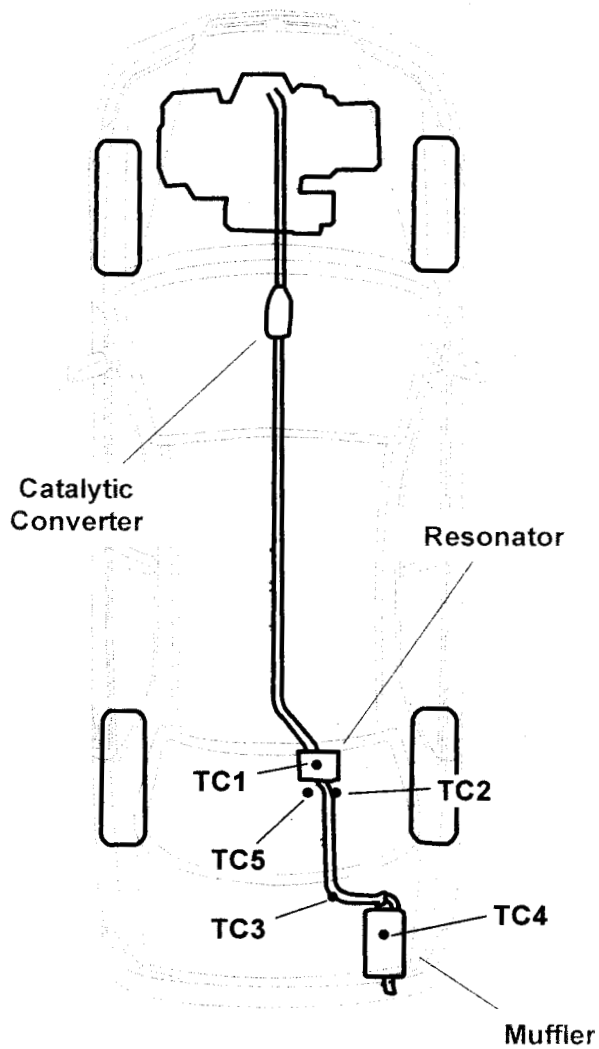

Figure D1. Crash Test C12611. Diagram showing the approximate locations of thermocouples on the exhaust system and the fuel tank / rear axle assembly in the test vehicle.

Thermocouple TC1 was intrinsically welded to the lower surface of the exhaust system resonator. Thermocouples TC2 and TC3 were intrinsically welded to Exhaust Pipe B. Thermocouple TC4 was intrinsically welded to the lower surface of the muffler. Thermocouple TC5 was a shielded thermocouple located near the rear surface of the resonator.

Each thermocouple was connected to a thermocouple amplifier (OMNI-AMP IV, Omega Engineering, Stamford, CT) calibrated using a thermocouple calibrator (Model CL27, Omega) at 0, 100, 200, 300, 400, 500, 600, 700, 800, 900, and 1000°C. The output signals from the thermocouple amplifiers were recorded by the data acquisition system at the crash test facility.

Plots D1 through D5 show temperature data recorded from thermocouples TC1 through TC5, respectively.

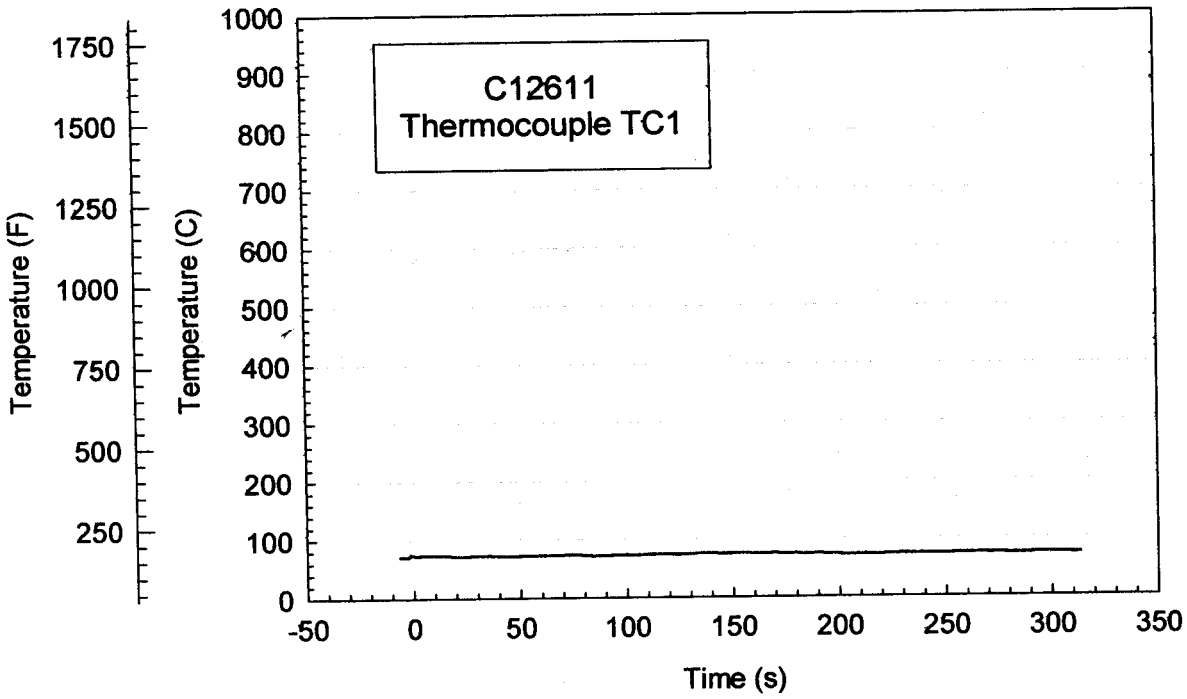

Plot D1. Crash Test C12611. Temperature data recorded from Thermocouple TC1.

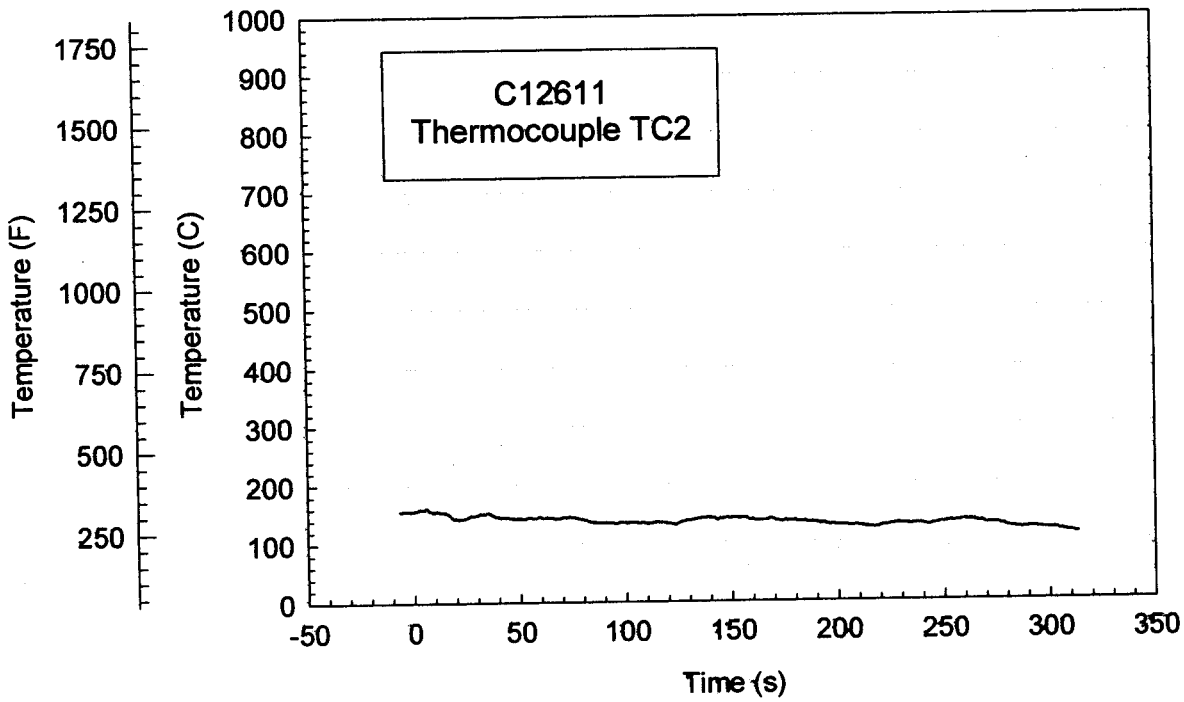

Plot D2. Crash Test C12611. Temperature data recorded from Thermocouple TC2.

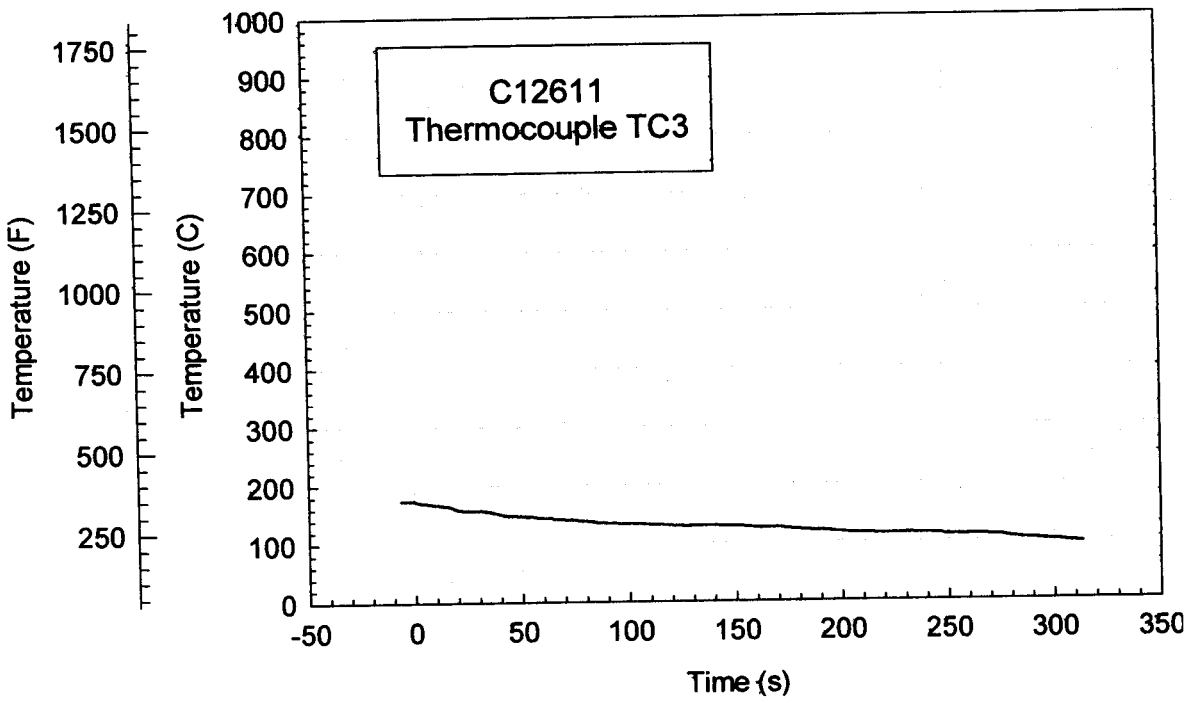

Plot D3. Crash Test C12611. Temperature data recorded from Thermocouple TC3.

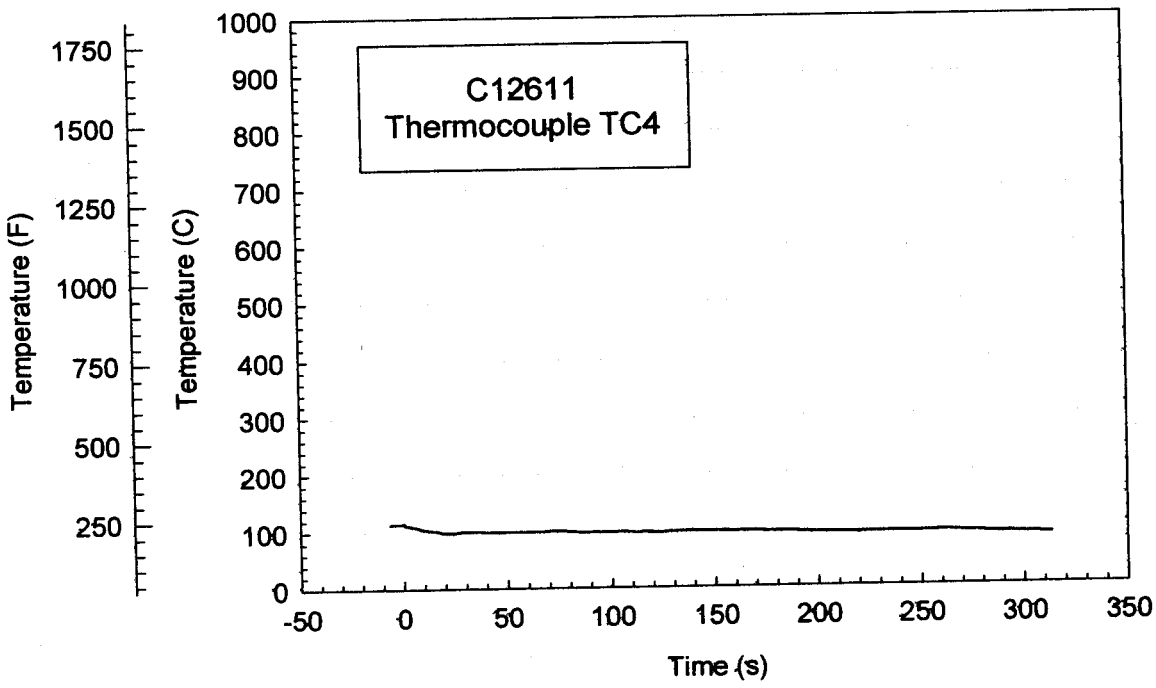

Plot D4. Crash Test C12611. Temperature data recorded from Thermocouple TC4.

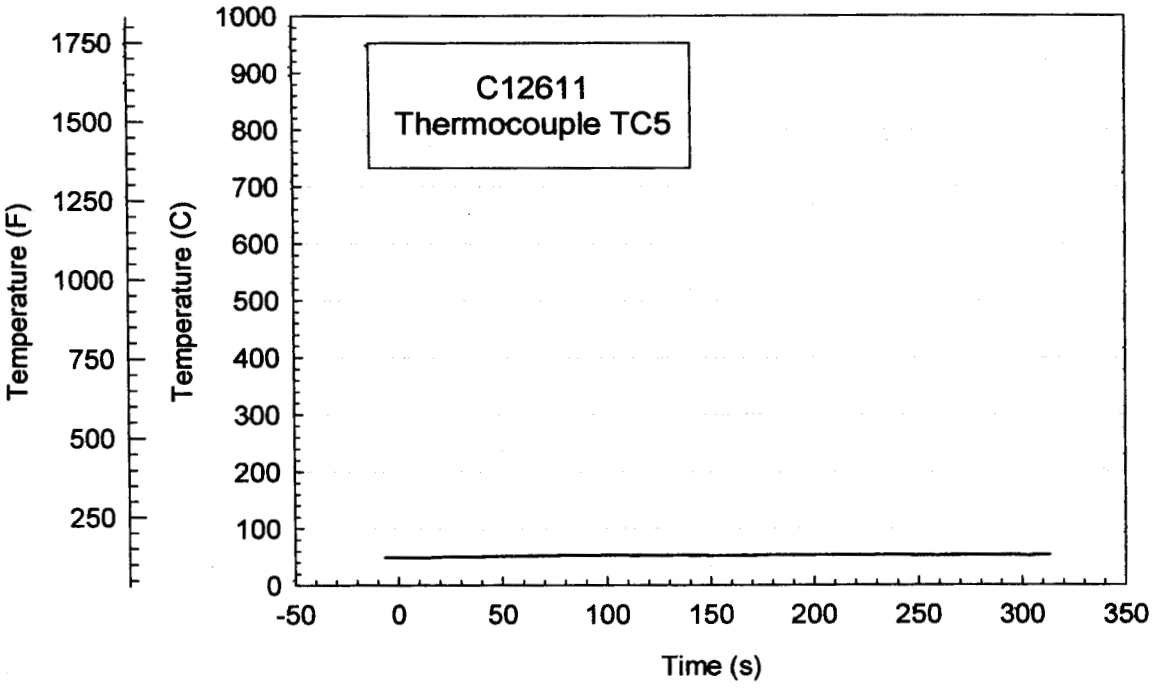

Plot D5. Crash Test C12611. Temperature data recorded from Thermocouple TC5.

Appendix E

Fire Suppression System

Crash Test C12610

The fire suppression system installed in the test vehicle for the tests described in this report included two solid propellant gas generator fire suppression units (Primex Aerospace Company, Redmond, WA) and two optical flame detectors (PM-3C Infrared Sensor, Santa Barbara Dual Spectrum, Goleta, CA). Figures E1 and E2 are photographs showing the locations of the SPGG units and optical flame detectors on the test vehicle before the crash test.

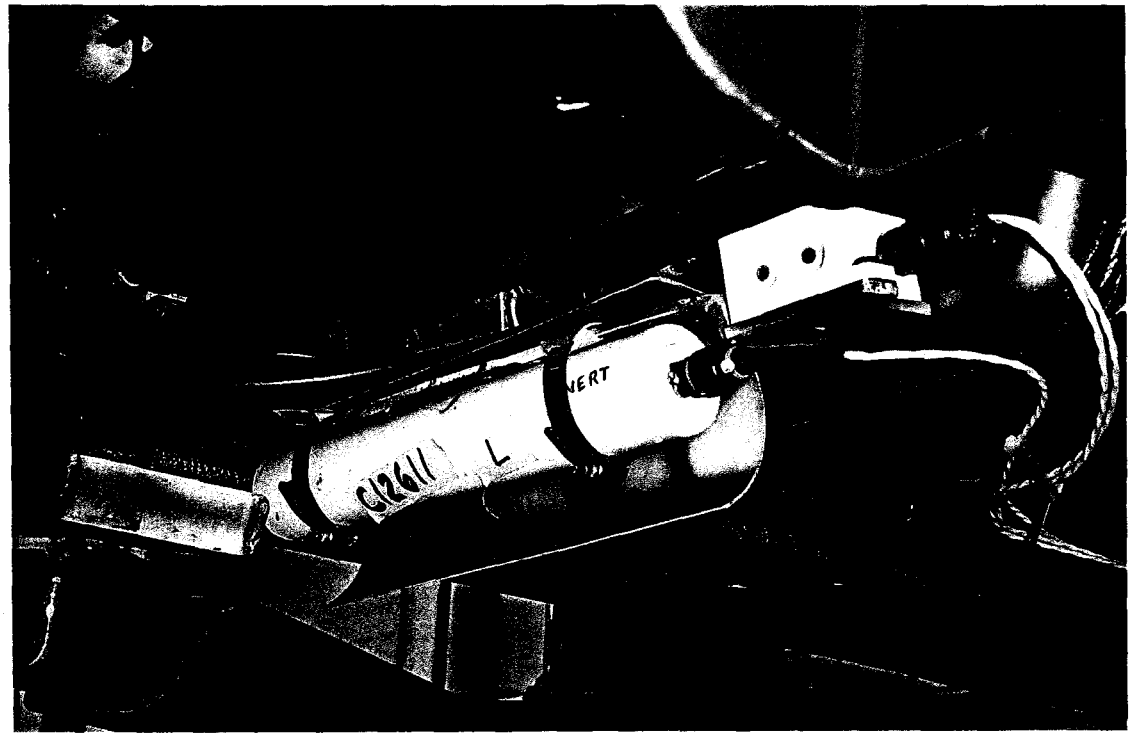

Figure E1. Crash Test C12611. Photograph showing the locations of the solid propellant gas generator flame suppression units and optical flame detectors on the left side of the test vehicle before the crash test. The rear of the test vehicle is to the left in this photograph.

Both SPGG units and optical flame detectors were mounted to the floor panel in the test vehicle in the "kick-up" area for the rear seat cushion. Each SPGG unit was attached to an aluminum bracket using two adjustable hose clamps. The aluminum brackets were bolted to the floor panel just inboard of the left and right rocker panels (Fig.'s E1 and E2). Each bracket contained a curved shield to direct the effluent from the SPGG unit toward the rear of the test vehicle and a platform for one optical flame detector. The optical flame detectors were aimed toward the rear of the test vehicle and angled downward approximately - 5° relative to the plane of the floor panel

Figure E2. Crash Test C12611. Photograph showing the locations of the solid propellant gas generator flame suppression units and optical flame detectors on the right side of the test vehicle before the crash test. The rear of the test vehicle is to the right in this photograph.

(Fig.'s E1 and E2). As shown in Figures E1 and E2, inert SPGG units were used to position the SPGG units and optical flame detectors in the test vehicle. These inert SPGG units were replaced with live SPGG units by a technical representative from the supplier of this equipment just before this crash test.

Signal leads from the SPGG units and optical flame detectors were connected to a programmable controller that was configured to activate both SPGG units if either optical flame detector sensed fire. The SPGG units, optical flame detectors, and programmable controller were designed for application in military aircraft and land vehicles and required a 24 VDC power supply. The test vehicle was equipped with a standard 12 VDC lead/acid automotive battery. Two 12 VDC dry cell batteries were connected in series to supply electrical power to the fire suppression system for this crash test.

The output signals from each optical flame detector (DETECTOR 1 = LEFT and DETECTOR 2 = RIGHT) and the firing signals to each SPGG unit (SPGG 1 = LEFT and SPGG 2 = RIGHT) were monitored and recorded during this crash test. Plots E1 and E2 show the outputs recorded from

these detectors from – 100 ms to + 500 ms post-impact, where the origin of the abscissa is the time of first contact between the moving barrier and the test vehicle determined by a linear contact strip on the bumper of the front test vehicle. Plots E3 and E4 show the firing signals to each SPGG unit.

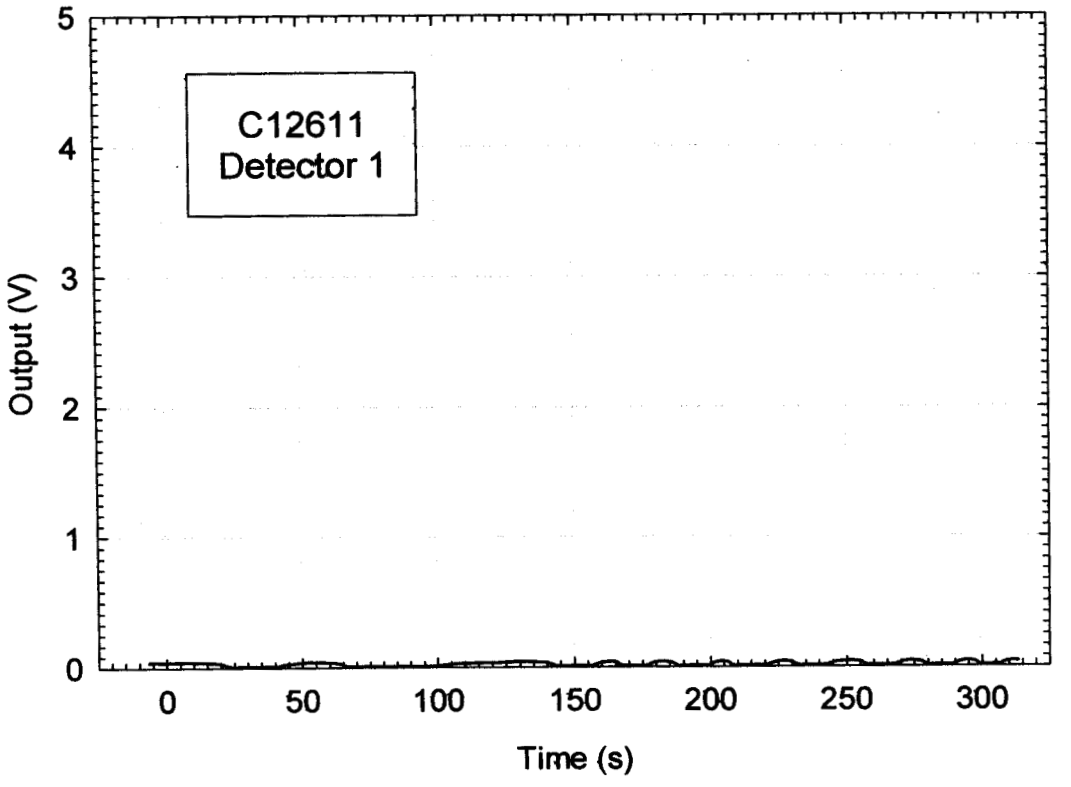

Plot B31. Crash Test C12611. Output from Optical Flame Detector 1.

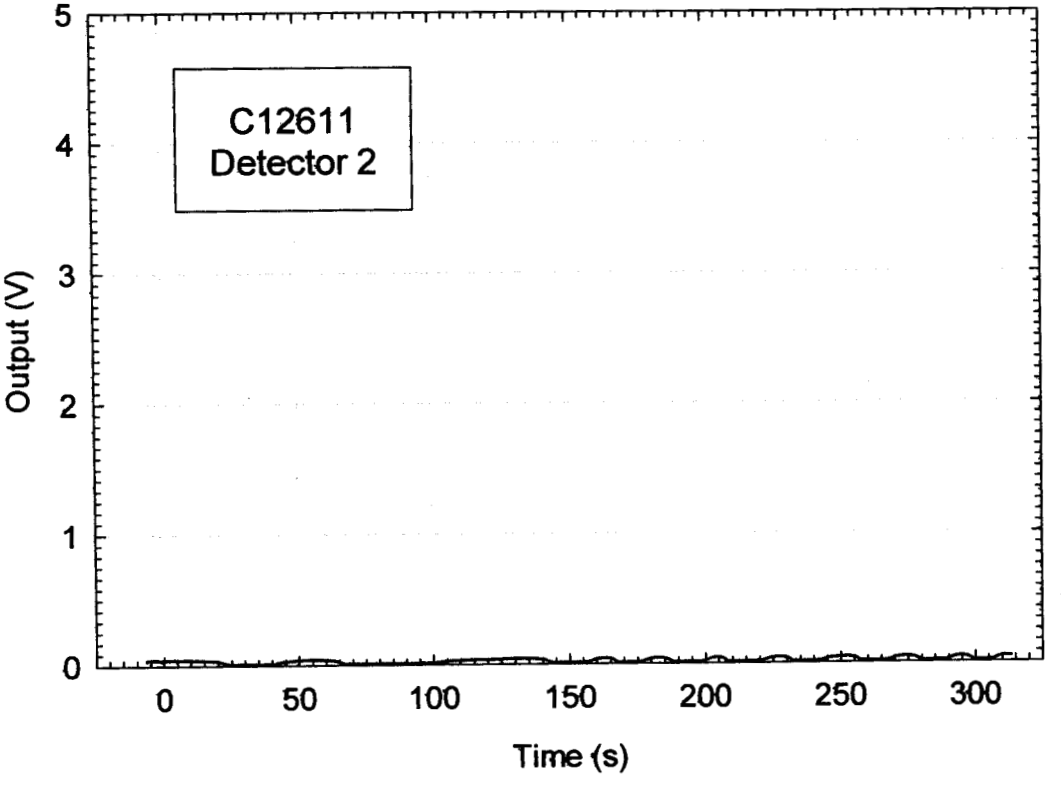

Plot B32. Crash Test C12611. Output from Optical Flame Detector 2.

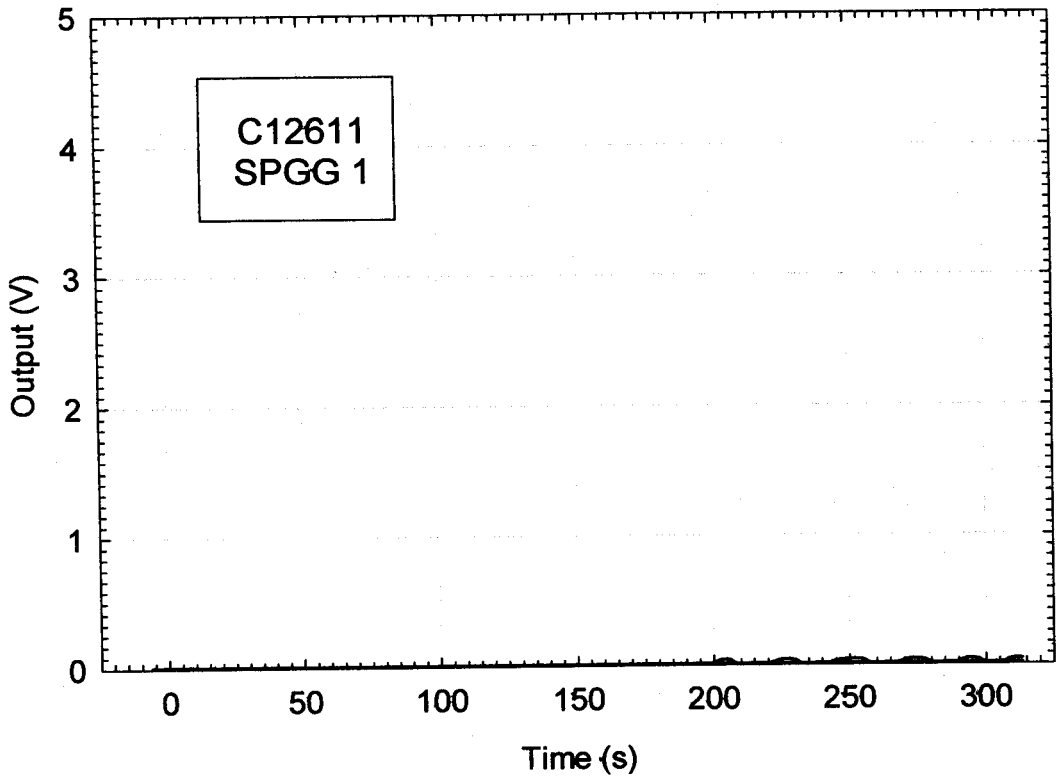

Plot B33. Crash Test C12611. Firing signal to SPGG 1.

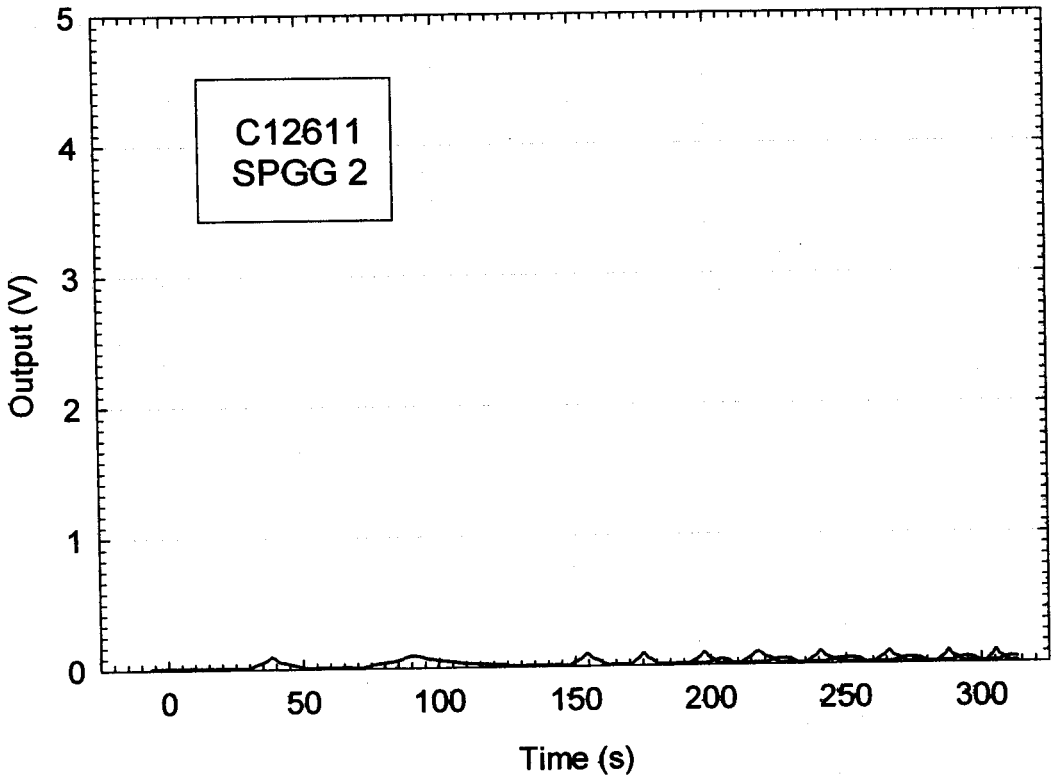

Plot B34. Crash Test C12611. Firing signal to SPGG 2.